A SCALAR DESCRIPTION OF ELEMENTARY WAVES IN ISOTROPIC ELASTIC MEDIA: MODELING AND MIGRATION

Jörg Schleicher and Martin Tygel

Wave Inversion Technology
Geophysical Institute, Uni Karlsruhe

Campinas, November 20, 1998

Wave Inversion Technoloty (WIT) Consortium Project, Dept. Applied Math.,
IMECC/UNICAMP, C.P. 6065, 13081-970 Campinas, SP, Brazil

Abstract

In the two chapters of this report, we take a closer look at the high-frequency approximations of two integrals associated with the name of Kirchhoff. The first one, dealt with in Chapter I, is the traditional Kirchhoff integral. It provides an integral representation of the seismic response at a receiver, given the locations of a source-receiver pair, a laterally inhomogeneous velocity model, and a reflector. On the use of the Kirchhoff-Helmholtz approximation for the reflected field at the reflector, an approximate forward modeling integral results that we call more appropriately the Kirchhoff-Helmholtz integral. The second integral, dealt with in Chapter II, is the more recent diffraction-stack integral also known as the Kirchhoff-migration integral. With it, the observed seismic response of an unknown reflector (recorded by an arbitrary source-receiver configuration) can be imaged into the reflector. This imaging is performed with the help of a laterally inhomogeneous macro-velocity model. As shown in Chapter II, both operations (i.e., the Kirchhoff-Helmholtz and the diffraction-stack integrals) can, under certain circumstances, be understood, both qualitatively and quantitatively, as being "physical inverse" operations to each other. In the same way as the Kirchhoff-Helmholtz integral can be conceived as a superposition of Huygens secondary sources distributed along a specified reflector, the diffraction-stack integral can be interpreted as a process that recovers the location and amplitude of the very same Huygens sources upon this reflector from their individual contributions to the seismic data, thus imaging the reflector together with its reflection coefficients. This explains mathematically why a diffraction-stack migration works.

CHAPTER I: FORWARD MODELING

Introduction

Wave phenomena are generally described by different wave equations. An important role in this respect plays the acoustic wave equation. Acoustic waves as well as the components of electromagnetic waves are described by this equation. Even a description of elastodynamic waves by an acoustic wave equation will be fairly accurate, whenever the compressional and shear components of the wavefield are sufficiently well decoupled (as in the case of ray theory). Different volume and surface integral solutions to the acoustic wave equation have been discussed by Wapenaar and Berkhout (1993). In this report, we deal with one of the surface integral solutions, namely the well-known Kirchhoff integral (Sommerfeld, 1964; Haddon and Buchen, 1981). It computes the propagation of waves away from the actual sources using the wavefield and its normal derivative on a closed surface encompassing the observation point in a constant-velocity medium. It can, as is well-known, be extended to the case of reflected waves in an inhomogeneous medium, which are propagated away from a reflecting or interface into the direction *towards* the (primary) sources. Following Huygens' principle, the reflected waves can be interpreted as being generated by "secondary sources" distributed along the specified reflector. Although mathematically not consistent and, therefore, obviously strictly not correct, it is often useful to insert the so-called "Kirchhoff-Helmholtz boundary conditions" (Sommerfeld, 1964) into the Kirchhoff integral. These conditions, which represent a generalization of the so-called physical-optics approximation for a perfectly soft or rigid reflector, replace the (unknown) total field on the illuminated portion of the reflector by the specularly reflected field that can be approximated by the (known) incident field multiplied by an appropriate plane-wave reflection coefficient. In the same way, the normal derivative of the specularly reflected field is approximated by the normal derivative of the incident field multiplied by the same reflection coefficient. At each point of the reflector, this reflection coefficient is computed under the assumption that the incident wavefield impinges upon the reflector locally as a plane wave, whereby the reflector is also replaced by its tangent plane at the incident point. Corresponding considerations are valid for the transmitted field and the respective transmission coefficient.

Inserting Kirchhoff-Helmholtz boundary conditions into the Kirchhoff integral provides in fact a high-frequency approximation to the reflected wave. This leads to what is referred to as the "Kirchhoff-Helmholtz approximation" (see also, e.g., Frazer and Sen, 1985). Therefore we call the resulting integral (which is considered in forward seismic modeling problems) briefly the "Kirchhoff-Helmholtz integral (KHI)." For modeling purposes, this celebrated integral is traditionally used to obtain the reflection response of a smooth reflector below a layered, smoothly varying overburden (in which ray theory applies). Though mostly formulated for a common-shot configuration, we present this integral here for arbitrary seismic measurement configurations.

In contrast to their usefulness in forward problems, neither the original Kirchhoff integral nor the KHI is suited for solving the inversion problem that aims at imaging the reflector and/or finding the interface-reflection coefficients. One way to solve the inversion problem for a common-shot record is to backward propagate the reflected wavefield (Schneider, 1978; Berkhout, 1985; Wapenaar, 1993). This can be done by a trick, namely by replacing in the Kirchhoff integral the retarded Green's functions by advanced ones, which leads to the Porter-Bojarski integral (Langenberg, 1986). In other words, the recorded reflected wave is restarted with Huygens waves at the measurement surface. In this way the reflected wave propagates back into the medium towards the secondary sources, i.e., towards the reflector. If considered in conjunction with the forward propagated field from the common source and a suitable imaging condition (Claerbout, 1971), the reflector can be imaged.

However, this approach does not work for seismic measurement configurations other than common-shot or common-receiver configurations (see Docherty, 1991). Another, more recent approach to image reflected waves, valid for arbitrary measurement configurations, is based on the geometrically motivated diffraction stack (Hagedoorn, 1954). Here, for each point in the given macro-velocity model, the amplitude values of the seismic traces are summed up along the corresponding diffraction traveltime surface and the obtained stack result is assigned to the chosen depth point. The mathematical formulation of this latter procedure in the high-frequency approximation (see, e.g., Bleistein, 1987; Schleicher et al., 1993) leads to the weighted "diffraction-stack integral (DSI)." The result of the DSI is the image of the subsurface reflector giving a measure of the reflection coefficient at any reflector location.

In this report, we try to give a physical meaning to the heuristic ansatz chosen for the DSI in Schleicher et al. (1993) by revealing its relationship to the KHI. We extend the acoustic case presented in Tygel et al. (1994a) to an elementary elastic wave. As shown in Chapter II, both the Kirchhoff-Helmholtz and the Kirchhoff-migration integrals give rise to closely related imaging operations. Although both integral representations are not exactly inverses to each other in an asymptotic sense, the DSI can be said to recover the information that is the input to the KHI. The proof of this fact will be given in Chapter II of this report.

Our analysis will lead us to the following physical interpretation of both integrals, which might be intuitively obvious but which will be mathematically quantified below. The KHI (here considered for a smooth reflector below a smooth laterally inhomogeneous overburden) is usually understood as the superposition of Huygens elementary waves located along the reflector and exploding (in response to the incident wave) with secondary-source strengths proportional to the local plane-wave reflection coefficients. Each Huygens source would, if exploding on its own, generate seismic energy distributed along the "diffraction-traveltime surface" (therefore also called "Huygens surface") in the seismic record that results from the selected measurement configuration. The envelope of these Huygens surfaces is the reflection-time surface. In other words, the two reflector attributes "location" and "reflection coefficient" are mapped by way of the Huygens sources into the recorded reflection within the seismic record section.

On the other hand, stacking the seismic trace amplitudes in the very same seismic record section along the diffraction-time surface that pertains to a Huygens secondary-source point involves then summing up all contributions that come from this particular Huygens wave center. This operation, which is done by the DSI with certain weights, recovers then again from the recorded reflection both the reflector location and the reflection coefficient, i.e., the two attributes that characterize the Huygens source. In this way, the DSI can be interpreted as being a "physical inverse" to the KHI.

The main emphasis in Chapter I is put on (a) reviewing the properties of the classical KHI, (b) formulating it for arbitrary measurement configurations, and (c) providing its asymptotic evaluation in such a way that it can be combined in Chapter II with an analogous treatment of the DSI. In this way, both integrals can then be viewed as an asymptotic integral pair which helps to understand the close relationship between forward modeling and migration/inversion.

Kirchhoff-Helmholtz integral

The classical Kirchhoff integral (see, e.g., Sommerfeld, 1964) represents a time-harmonic acoustic wavefield $\hat{U}(G,\omega)$ (e.g., the pressure or the principal component of the elastic displacement vector) at the observation point G (that is, the receiver location) in a constant-velocity medium in terms of that very field, $\hat{U}(P,\omega)$, and its normal derivative, known at all points P on a given smooth surface Σ_0 that encloses point G (Figure I.1), provided the sources from which the field $\hat{\Phi}(P,\omega)$ originated are located outside Σ_0. It also uses the Green's function $\hat{\mathcal{G}}(P,G,\omega)$, as well as

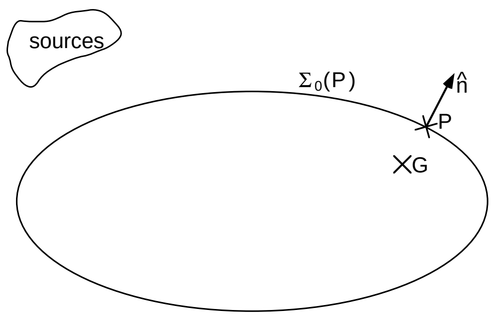

Fig. I.1. The Kirchhoff integral computes the wavefield at an observation point (receiver) G provided the field and its normal derivative are given at an arbitrary surface Σ_0 surrounding G. The sources of the field must be outside Σ_0. For simplicity, the 3-D situation is featured by a 2-D sketch.

its normal derivative, computed at all points P on Σ_0 for a hypothetical fixed point source at G. The symbol ω in the above expressions stands for a positive circular frequency. The time-harmonic dependency $\exp(i\omega t)$ is omitted in all expressions below.

With this understanding, the standard Kirchhoff integral (see, e.g., Langenberg, 1986) may be written as

$$\hat{U}(G,\omega) \;=\; \frac{1}{4\pi}\iint\limits_{\Sigma_0} d\Sigma_0(P)\frac{1}{\rho(P)}\;\left[\hat{U}(P,\omega)\frac{\partial\hat{\mathcal{G}}}{\partial n}(G,P,\omega)-\hat{\mathcal{G}}(G,P,\omega)\frac{\partial\hat{U}}{\partial n}(P,\omega)\right]\;, \tag{I.1}$$

where the vector $\hat{\boldsymbol{n}}$, normal to Σ_0, points *outwards*, i.e., out of the enclosing surface Σ_0 into the region where the sources of the wavefield $\hat{U}(G,\omega)$ are found. Also, $\partial/\partial n = \hat{\boldsymbol{n}}\cdot\boldsymbol{\nabla}$ denotes the normal derivative in that direction. Finally, $\rho(P)$ is the density of the medium at point P.

As shown in Appendix A, elementary elastic waves can be described by a scalar wave equation, too. In Appendix B, we derive the corresponding scalar elastic Kirchhoff integral. From this Appendices, we see that a similar scalar description holds not only for acoustic but also for elementary elastic waves. All we have to do is to introduce a medium parameter function $f(P)$ which varies with the location of P. For acoustic waves, $f = 1/\rho$ and for elastic waves, $f = \rho v^2$, where v is the local wave velocity at P. In this generalization, we have the following form of the scalar Kirchhoff integral

$$\hat{U}(G,\omega) \;=\; \frac{1}{4\pi}\iint\limits_{\Sigma_0} d\Sigma_0(P)\;f(P)\;\left[\hat{U}(P,\omega)\frac{\partial\hat{\mathcal{G}}}{\partial n}(G,P,\omega)-\hat{\mathcal{G}}(G,P,\omega)\frac{\partial\hat{U}}{\partial n}(P,\omega)\right]\;. \tag{I.2}$$

By letting a part of the enclosing surface Σ_0 coincide with the illuminated portion of a reflecting interface (see Figure I.2) and by extending the rest of Σ_0 towards infinity and applying

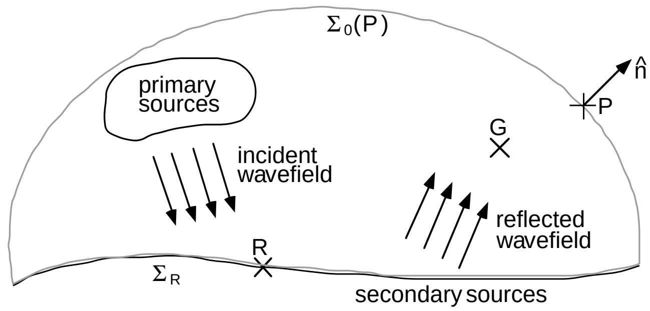

FIG. I.2. For the computation of the reflected field at G, surface Σ_0 is extended to match the reflector Σ_R at one side and to approach infinity everywhere else. For simplicity, the 3-D situation is featured by a 2-D sketch.

Sommerfeld's radiation condition, the Kirchhoff integral (I.2) can be used to describe the field scattered from the reflecting interface (see, e.g., Bleistein, 1984). Note that the primary sources are now assumed to lie inside Σ_0 so that the incident (or direct) wavefield is not propagated by integral (I.2), whereas the secondary sources (scatterers) are assumed to be outside Σ_0 (Figure I.2). In the following, the illuminated part of the reflecting interface is denoted by Σ_R. As is shown in Appendix B, a corresponding procedure can also be conceived for the transmission case. Thus, all following derivations, although discussed with respect to a reflected wavefield, can also be applied to a transmitted wavefield.

Let us now assume that the wavefield to be described results form an omnidirectional point source at a point S. This source emanates a signal described by a function $F[t]$. Denoting the Green's function of the scattered field originating from a point source at S by $\hat{\mathcal{G}}^s$, we have $\hat{U} = \hat{F}[\omega]\hat{\mathcal{G}}^s$. Thus, the Kirchhoff integral for a laterally inhomogeneous overburden can be written as an integration over all points $P = R$ of the surface Σ_R, viz.,

$$\hat{U}(G,\omega) = \frac{-\hat{F}[\omega]}{4\pi} \iint_{\Sigma_R} d\Sigma_R(R)\; f(R)\; \left[\hat{\mathcal{G}}^s(S,R,\omega)\; \frac{\partial\hat{\mathcal{G}}(G,R,\omega)}{\partial n} - \frac{\partial\hat{\mathcal{G}}^s(S,R,\omega)}{\partial n}\; \hat{\mathcal{G}}(G,R,\omega)\right] . \quad \text{(I.3)}$$

The different sign in comparison to equation (I.2) accounts for the inverted direction of $\hat{\boldsymbol{n}}$. In fact it is common in the literature to invert the direction of the surface normal during this process so as to have it pointing *towards* the observation point G.

The Kirchhoff-Helmholtz approximation replaces the (unknown) Green's function $\hat{\mathcal{G}}^s(S,R,\omega)$ of the scattered field in equation (I.3) at each point $P = R$ on the reflecting interface Σ_R by the following (known) single-scattering approximation of the specularly reflected field (Figure I.2). It can be understood as a local plane-wave approximation due to its analogies to the reflection of a plane wave at a planar interface as explained in Appendix C. To obtain the approximate reflected wavefield, let the reflector at R be locally replaced by its tangent plane. Also, suppose that the incident field is replaced by a plane wave with the same frequency, amplitude, and incidence angle as the actually incident wave at R. Immediately after reflection, the approximate reflected field is equal to the incident field multiplied by the plane-wave reflection coefficient $R_c(R)$. The propagation direction of the reflected wavefield is determined by Snell's law. In other words, both the wave vector and the reflection coefficient of the reflected wave are determined by the incident field and the normal direction of reflection surface Σ_R. In the same way, the normal derivative of the reflected field is replaced by the normal derivative of the local plane-wave reflection at R. Due to the different propagation directions before and after specular reflection, the specular reflected field at R has the *same* sign as the incident field whereas its normal derivative has *opposite* sign. The indicated procedure is a natural generalization of the physical optics approximation (see, e.g., Bleistein, 1984; or Langenberg, 1986), where the above substitutions are made for perfectly rigid ($R_c = 1$) or perfectly soft ($R_c = -1$) scatterers Σ_R.

In symbols, we have for the scattered field $\hat{\mathcal{G}}^s(S,R,\omega)$ in Kirchhoff-Helmholtz approximation (see also Appendix C)

$$\hat{\mathcal{G}}^s(S,R,\omega) = R_c(R)\,\hat{\mathcal{G}}(S,R,\omega)\ , \tag{I.4a}$$

$$\frac{\partial\hat{\mathcal{G}}^s(S,R,\omega)}{\partial n} = i\omega\,\frac{\cos\alpha_R^+}{v_R^+}\,R_c(R)\,\hat{\mathcal{G}}(S,R,\omega)\ , \tag{I.4b}$$

where $\hat{\mathcal{G}}(S,R,\omega)$ is the Green's function of the incident wavefield at R and $R_c(R)$ denotes the plane-wave reflection coefficient at point R on the interface Σ_R, given the ray incident from the source at S. Moreover, v_R^+ is the medium velocity at point R that governs the wave propagation after reflection. Finally, α_R^+ in equation (I.4b) denotes the acute angle which the specular reflected ray makes with the normal $\hat{\boldsymbol{n}}$ to Σ_R at R immediately *after* reflection at R on Σ_R (see Figure I.3). In other words, it is connected to the incidence angle α_R^- at R via Snell's law. Note that the above

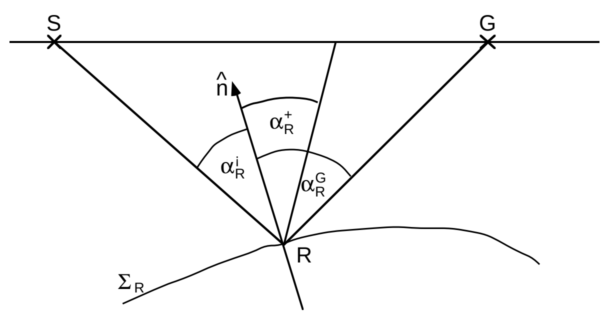

FIG. I.3. Geometric situation at the reflector. The angles α_R^-, α_R^+, and α_R^G at R denote the incidence angle of the ray from S, the angle of specular reflection, and the angle of the nonspecular ray to G, respectively. For details, see text. In this 2-D sketch featuring the 3-D situation, a constant-velocity medium and a planar measurement surface are used for simplicity.

representation for $\hat{\mathcal{G}}^s(S,R,\omega)$ is a high-frequency approximation for the field scattered from Σ_R which is equivalent to zero-order ray theory (see also Appendix C).

Two Green's functions $\hat{\mathcal{G}}(S,R,\omega)$ and $\hat{\mathcal{G}}(G,R,\omega)$ (i.e., the time-harmonic responses at R for point-sources at S and G, respectively) are, in general, very difficult to obtain analytically in inhomogeneous media. They are, thus, in analogy to the above high-frequency approximation for $\mathcal{G}^s(S,R,\omega)$, in most computations replaced by their leading terms in powers of $1/\omega$, i.e., by their zero-order ray-theoretical (high-frequency) approximations

$$\hat{\mathcal{G}}(S,R,\omega) \simeq \mathcal{G}_0(S,R)\ \exp[-i\omega\tau(S,R)] \tag{I.5a}$$

and

$$\hat{\mathcal{G}}(G,R,\omega) \simeq \mathcal{G}_0(G,R)\ \exp[-i\omega\tau(G,R)], \tag{I.5b}$$

where $\mathcal{G}_0(G,R)$ and $\tau(G,R)$ denote the amplitude factor and traveltime along the ray GR, with corresponding meanings for $\mathcal{G}_0(S,R)$ and $\tau(S,R)$. As explained in Appendix C, the use of the

Kirchhoff-Helmholtz approximation is equivalent to further consider the high-frequency approximations of the normal derivative of the Green's function $\hat{\mathcal{G}}(G,R,\omega)$,

$$\begin{aligned}
\frac{\partial \hat{\mathcal{G}}(G,R,\omega)}{\partial n} &= \frac{\partial}{\partial n}\Big[\mathcal{G}_0(G,R)\exp[-i\omega\tau(G,R)]\Big] \\
&= [\frac{\partial \mathcal{G}_0(G,R)}{\partial n} + \mathcal{G}_0(S,R)\ (-i\omega)\ \frac{\partial \tau(G,R)}{\partial n}]\ \exp[-i\omega\tau(G,R)] \\
&\simeq (-i\omega)\ \frac{\partial \tau(G,R)}{\partial n}\ \mathcal{G}_0(G,R)\ \exp[-i\omega\tau(G,R)] \\
&\simeq (-i\omega)\ \frac{\cos\alpha_R^G}{v_R^+}\ \mathcal{G}_0(G,R)\ \exp[-i\omega\tau(G,R)]\ . \qquad \text{(I.6)}
\end{aligned}$$

Here, α_R^G denotes the acute angle the ray GR makes with the normal to Σ_R at R (see Figure I.3). The last equality in equation (I.6) can be readily derived using the eikonal equation for the ray GR.

Equations (I.4) together with (I.5) and (I.6) constitute the Kirchhoff-Helmholtz approximation and correspond to equations (C-9) and (C-10) in Appendix B. The expression resulting from inserting these high-frequency expressions into the Kirchhoff integral of equation (I.2) is called the "Kirchhoff-Helmholtz integral (KHI)." Using a slightly modified notation, we find for the KHI the important expression

$$\hat{U}(G,\omega) \simeq \hat{F}[\omega]\frac{i\omega}{2\pi}\iint_{\Sigma_R} d\Sigma_R(R)\, R_c(R)\, K_{KH}(S,R,G)\ \exp[-i\omega\tau_D(S,R,G)], \qquad \text{(I.7a)}$$

or in the time domain

$$U(G,t) \simeq \frac{1}{2\pi}\iint_{\Sigma_R} d\Sigma_R(R)\, R_c(R)\, K_{KH}(S,R,G)\ F'[t-\tau_D(S,R,G)]\ , \qquad \text{(I.7b)}$$

where the prime denotes the derivative with respect to the argument. In this case, this is equal to the time derivative. The *point-diffractor traveltime* $\tau_D(S,R,G)$ in formulas (I.7) is simply the sum of the traveltimes along the rays SR and GR, namely,

$$\tau_D(S,R,G) = \tau(S,R) + \tau(G,R). \qquad \text{(I.8)}$$

It can be associated with the traveltime of a "diffraction event" from the source at S to the hypothetical Huygens secondary-source point R on Σ_R and from there to the observation point G. The *amplitude kernel* $K_{KH}(S,R,G)$ is given by

$$K_{KH}(S,R,G) = f(R)\ \mathcal{G}_0(S,R)\ \mathcal{G}_0(G,R)\ \mathcal{O}_{KH}(S,R,G), \qquad \text{(I.9)}$$

in which $\mathcal{O}_{KH}(S,R,G)$ denotes the so-called *obliquity factor*

$$\mathcal{O}_{KH}(S,R,G) = \frac{\cos\alpha_R^+ + \cos\alpha_R^G}{2v_R^+}\ . \qquad \text{(I.10)}$$

The obliquity factor $\mathcal{O}_{KH}(S,R,G)$ accounts for the difference in directions of the specular reflected ray and ray GR at R.

Let us now assume that the reflecting interface Σ_R is given in a parametrized form with a 2-D parameter vector, say $\boldsymbol{\eta}$. In other words, we set $R = R(\boldsymbol{\eta})$. Moreover, we assume that the considered source and observation points lie on a given measurement surface Σ_M and that to each source point S there corresponds one receiver point G. In that case, also S and G can be expressed in parametrized form with a 2-D parameter vector, say $\boldsymbol{\xi}$. In other words, we write $S = S(\boldsymbol{\xi})$ and $G = G(\boldsymbol{\xi})$. Using these parametrizations, we can recast the KHI representations (I.7a) (in the frequency domain) and (I.7b) (in the time domain) into

$$\hat{U}(\boldsymbol{\xi},\omega) \simeq \frac{i\omega}{2\pi}\,\hat{F}[\omega] \iint\limits_{\Sigma_R} d\Sigma_R(\boldsymbol{\eta})\; K_{KH}(\boldsymbol{\xi},\boldsymbol{\eta})\; R_c(\boldsymbol{\eta})\; \exp[-i\omega\tau_D(\boldsymbol{\xi},\boldsymbol{\eta})], \tag{I.11a}$$

and

$$U(\boldsymbol{\xi},t) \simeq \frac{1}{2\pi} \iint\limits_{\Sigma_R} d\Sigma_R(\boldsymbol{\eta})\; K_{KH}(\boldsymbol{\xi},\boldsymbol{\eta})\; R_c(\boldsymbol{\eta})\; F'[t-\tau_D(\boldsymbol{\xi},\boldsymbol{\eta})], \tag{I.11b}$$

respectively. All quantities within the integrands of these two integrals are now functions of $\boldsymbol{\xi}$ and $\boldsymbol{\eta}$ and not any more of S, R and G. It is worthwhile to keep in mind that in the KHI, the vector $\boldsymbol{\xi}$ remains fixed and only $\boldsymbol{\eta}$ varies. Note that in Appendix D, integral (I.11a) is obtained independently from applying the elastic generalization of the Kirchhoff-Helmholtz approximation to the full elastic, anisotropic representation integral, and reducing the resulting expression to the case of isotropy.

Introducing the notation

$$u(\boldsymbol{\eta},t) = R_c(\boldsymbol{\eta})\; F[t]\;, \tag{I.12}$$

which we will identify as a quite natural description of a secondary Huygens source at $R(\boldsymbol{\eta})$ with $R_c(\boldsymbol{\eta})$ being the "Huygens source strength" and with the "Huygens source wavelet" given by $F[t]$, the above expression (I.11b) assumes the convenient compact form

$$U(\boldsymbol{\xi},t) \simeq \frac{1}{2\pi} \iint\limits_{\Sigma_R} d\Sigma_R(\boldsymbol{\eta})\; K_{KH}(\boldsymbol{\xi},\boldsymbol{\eta})\; \frac{\partial u}{\partial t}(\boldsymbol{\xi},\boldsymbol{\eta},t-\tau_D(\boldsymbol{\xi},\boldsymbol{\eta})) \tag{I.13}$$

that is suitable to be used in forward modeling and which is appropriate for the later treatment. For convenience, we introduce the notation

$$U(\boldsymbol{\xi},t) = I_{KH}[u(\boldsymbol{\eta},t)](\boldsymbol{\xi},t) \tag{I.14}$$

to represent the above integral (I.13).

Usually, the Kirchhoff integral (I.2) or its time-domain equivalent is interpreted as follows. The wavefield recorded at receiver G is constructed by a superposition of the contributions of monopole ($\hat{\mathcal{G}}(G,P,\omega)$) and dipole ($\hat{\partial}\mathcal{G}(G,P,\omega)/\partial n$) Huygens secondary sources originating at $d\Sigma_0(P)$ on the surface Σ_0 being excited by the incident field ($\hat{U}(P,\omega)$). The Kirchhoff-Helmholtz integral (I.13), on the other hand, gives a more compact representation. Here, the time-domain contributions of the monopoles and dipoles are combined. They are moreover separated into effects due to the overburden and the reflector. All overburden effects are accounted for by the integral kernel (we may also call it a weight function) $K_{KH}(\boldsymbol{\xi},\boldsymbol{\eta})$ and the time-function $\tau_D(\boldsymbol{\xi},\boldsymbol{\eta})$. The reflector attribute "location" is included in the integration over Σ_R and the quantity $u(\boldsymbol{\eta},t)$ accounts for the reflector attribute "reflection coefficient" $R_c(\boldsymbol{\eta})$. The question why $u(\boldsymbol{\eta},t)$ also includes the analytic source pulse $F[t]$ will be answered in the next paragraph.

Surely in formula (I.13) all quantities on the right-hand side are known and the separation of the integrand into overburden and reflector effects appears artificial. This is, however, no longer the case when the inverse problem is to be addressed. Like in forward modeling, also in inversion the overburden will be known on account of the macro-velocity model and the measurement configuration. The integral kernel $K_{KH}(\boldsymbol{\xi},\boldsymbol{\eta})$ and the time $\tau_D(\boldsymbol{\xi},\boldsymbol{\eta})$ can therefore be looked upon as the known parameters governing both modeling and inversion. On the other hand, the attributes of the reflector together with the source wavelet, being the "input" for modeling using the KHI, are the desirable unknown "output" of an inversion. In the same way, the seismic reflections, that are the "output" of modeling, are the "input" of an inversion. In other words, the Huygens sources map the reflector attributes and the source wavelet – which can therefore viewed as being attributes that characterize the Huygens sources as indicated in connection with equation (I.12) – into the seismic reflection. The inversion aims at recovering these attributes.

Asymptotic evaluation of the KHI

We return now to the KHI in the frequency domain (I.11a) and apply the stationary-phase method (Bleistein, 1984) to obtain its high-frequency asymptotic evaluation

$$\hat{U}(\boldsymbol{\xi},\omega) \simeq \Gamma_{KH}(\boldsymbol{\xi})\; R_c(\boldsymbol{\eta}_{Ref})\; \hat{F}[\omega]\; \exp[-i\omega\tau_D(\boldsymbol{\xi},\boldsymbol{\eta}_{Ref})]\;, \tag{I.15a}$$

where

$$\Gamma_{KH}(\boldsymbol{\xi}) = \frac{K_{KH}(\boldsymbol{\xi},\boldsymbol{\eta}_{Ref})}{|\det(\underset{\sim}{\boldsymbol{H}}_F(\boldsymbol{\xi}))|^{1/2}}\; \exp\left\{ i\frac{\pi}{4}[2-\mathrm{Sgn}(\underset{\sim}{\boldsymbol{H}}_F(\boldsymbol{\xi}))]\right\} \tag{I.15b}$$

with $\mathrm{Sgn}(\underset{\sim}{\boldsymbol{H}}_F)$ denoting the signature (number of positive eigenvalues minus number of negative eigenvalues) of the Hessian matrix

$$\underset{\sim}{\boldsymbol{H}}_F(\boldsymbol{\xi}) = \left.\left(\frac{\partial^2\tau_D}{\partial\eta_i\partial\eta_j}\right)\right|_{\boldsymbol{\eta}=\boldsymbol{\eta}_{Ref}} . \tag{I.16}$$

This matrix is supposed to be nonsingular (i.e., to have a nonvanishing determinant) throughout this work. In other words, receivers at caustic points are excluded from the present analysis. As shown in Hubral et al. (1992), matrix $\underset{\sim}{\boldsymbol{H}}_{Ref}(\boldsymbol{\xi})$ accounts for the influence of the Fresnel zone at the reflector on the reflected wavefield.

Transforming result (I.15a) back into the time domain, we find the following asymptotic result of the Kirchhoff-Helmholtz integral (I.14)

$$\begin{aligned} I_{KH}[u(\boldsymbol{\eta},t)](\boldsymbol{\xi},t) &= U(\boldsymbol{\xi},t) \\ &\simeq \Gamma_{KH}(\boldsymbol{\xi})\; R_c(\boldsymbol{\eta}_{Ref})\; F[t-\tau_D(\boldsymbol{\xi},\boldsymbol{\eta}_{Ref})]\;. \end{aligned} \tag{I.17}$$

In the above equations, $\boldsymbol{\eta}=\boldsymbol{\eta}_{Ref}$ is the stationary phase point of integral (I.11a), i.e., the one, where

$$\left.\frac{\tau_D(\boldsymbol{\xi},\boldsymbol{\eta})}{\partial\eta_i}\right|_{\boldsymbol{\eta}_{Ref}} = 0 \qquad \text{for } i=1,2\;. \tag{I.18}$$

It determines the reflection point $R_{Ref}=R(\boldsymbol{\eta}_{Ref})$ on Σ_R that pertains to the source-receiver pair $(S(\boldsymbol{\xi}),G(\boldsymbol{\xi}))$, so that SRG constitutes the reflection ray. As stated earlier, we assume that this ray is uniquely determined for the domains of definition of the parameter vectors $\boldsymbol{\xi}$ and $\boldsymbol{\eta}$ that describe the measurement configuration on Σ_M and the reflector Σ_R, respectively. In other words, equation (I.18) defines a one-to-one relationship between $\boldsymbol{\xi}$ and $\boldsymbol{\eta}_{Ref}=\boldsymbol{\eta}_{Ref}(\boldsymbol{\xi})$.

The important formula (I.17) possesses the form of the zero-order ray-theory solution of the reflection event that pertains to the source-receiver pair $(S(\boldsymbol{\xi}), G(\boldsymbol{\xi}))$. Let us now write representation (I.17) in the familiar ray-theoretical form

$$U(\boldsymbol{\xi}, t) = U_0(\boldsymbol{\xi})\; F[t - \tau_{Ref}(\boldsymbol{\xi})], \tag{I.19a}$$

where the amplitude factor is given by

$$U_0(\boldsymbol{\xi}) = R_c(\boldsymbol{\eta}_{Ref})\; \frac{\mathcal{A}(\boldsymbol{\xi})}{\mathcal{L}(\boldsymbol{\xi})}. \tag{I.19b}$$

In the above expression, $\tau_{Ref}(\boldsymbol{\xi})$ is the traveltime along the reflection ray SRG. Moreover, the factor $\mathcal{A}$ accounts for the amplitude loss due to crossing of overburden interfaces (transmission losses) along the total ray path excluding the reflection coefficient $R_c(\boldsymbol{\eta}_{Ref})$ at the interface Σ_R. For elastic elementary waves, it is given by (Červený, 1987)

$$\mathcal{A}(\boldsymbol{\xi}) = g\left[\frac{1}{\rho_S v_S^2 \rho_G v_G^2}\right]^{1/2} \prod_{n=1}^{N}\left[\frac{\rho_n^o v_n^o \cos\alpha_n^o}{\rho_n^i v_n^i \cos\alpha_i^o}\right]^{1/2} c_n = g\left[\frac{1}{\rho_S v_S^2 \rho_G v_G^2}\right]^{1/2} \prod_{n=1}^{N} \tilde{c}_n\;, \tag{I.20a}$$

where $\rho_n^{i,o}$, $v_n^{i,o}$, and $\alpha_n^{i,o}$ denote the density, wave velocity, and propagation angle, respectively, of the incoming and outgoing ray at the nth interface and c_n is the transmission coefficient at that interface. Also, g is the source strength that may include source directivity and radiation pattern factors. Note that the above expression for $\mathcal{A}$ is completely reciprocal as $\tilde{c}_n$ denotes the reciprocal transmission coefficient (Červený, 1987). For acoustic waves, we have correspondingly

$$\mathcal{A}(\boldsymbol{\xi}) = g\,[\rho_S \rho_G]^{1/2} \prod_{n=1}^{N}\left[\frac{\rho_n^i v_n^i \cos\alpha_n^o}{\rho_n^o v_n^o \cos\alpha_i^o}\right]^{1/2} c_n = g\,[\rho_S \rho_G]^{1/2} \prod_{n=1}^{N} \tilde{c}_n\;, \tag{I.20b}$$

Finally, in both cases the (real or imaginary) quantity

$$\mathcal{L}(\boldsymbol{\xi}) = \sqrt{\frac{J}{v_S v_G}} \tag{I.21}$$

denotes the *normalized reciprocal geometrical-spreading factor* of the total reflection ray SRG with J being the ray Jacobian. For a homogeneous medium, $\mathcal{L}$ equals the distance between source and receiver along the ray. The particular definition for $\mathcal{L}$ was chosen because it is a natural reciprocal extension to heterogeneous media of the normalized geometrical-spreading factor defined by Newman (1973) for horizontally layered media. The definition of Červený (1987) without velocity normalization is reciprocal but not a length, and the definition of Ursin (1990; also used in previous works of the authors, see, e.g., Schleicher et al., 1993) with normalization by the source velocity v_S is not reciprocal.

Equation (I.19a) is the final asymptotic result of the KHI. It states (in the high-frequency approximation) that the superposition of the contributions of all Huygens secondary sources originating along the reflector, each of which would distribute its energy along a diffraction traveltime surface $\tau_D(\boldsymbol{\xi}, \boldsymbol{\eta})$, constructively interferes and results in the total elementary wavefield reflected from Σ_R. The seismic reflection event resulting from this constructive interference in the $(\boldsymbol{\xi}, t)$-domain aligns itself along the reflection traveltime surface $\tau_{Ref}(\boldsymbol{\xi})$ (Figure I.4).

Geometrical-spreading decomposition

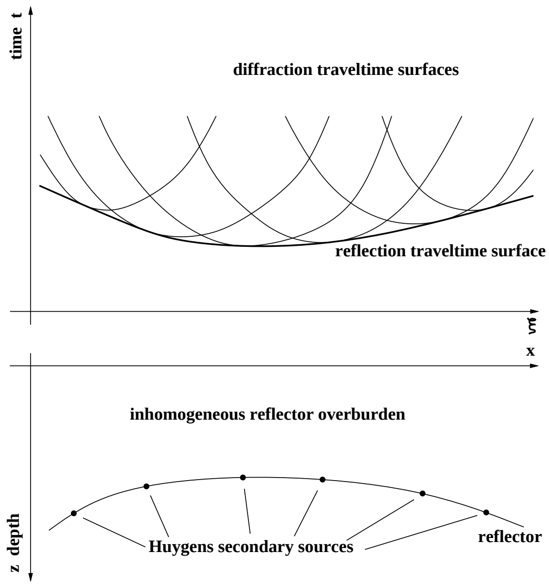

FIG. I.4. Physical interpretation of the Kirchhoff-Helmholtz integral (2-D sketch): Each Huygens secondary source, when exploding after excitation, produces energy in a seismic section along certain diffraction-traveltime surfaces. Superposing at the receiver the responses of all Huygens sources distributed along the reflector results in the usual elementary seismic reflection response with energy distributed along the reflection traveltime surface.

By the uniqueness of the ray solution, we may equate the right-hand-sides of expressions (I.17) and (I.19a) to obtain the relationships (Goldin, 1991; Schleicher et al., 1993)

$$\tau_{Ref}(\boldsymbol{\xi}) = \tau_D(\boldsymbol{\xi}, \boldsymbol{\eta}_{Ref}) \tag{I.22a}$$

for the traveltime and

$$\frac{\mathcal{A}(\boldsymbol{\xi})}{\mathcal{L}(\boldsymbol{\xi})} = \Gamma_{KH}(\boldsymbol{\xi}) \tag{I.22b}$$

for the amplitude of the wavefield at G.

Equation (I.22a) tells us the obvious fact that the total traveltime $\tau_{Ref}(\boldsymbol{\xi})$ along the reflection ray $SR_{Ref}G$ equals the sum of the traveltimes $\tau_D(\boldsymbol{\xi}, \boldsymbol{\eta}_{Ref})$ along the two ray segments, one from $S(\boldsymbol{\xi})$ to $R_{Ref}(\boldsymbol{\eta}_{Ref})$ and the other from $G(\boldsymbol{\xi})$ to this reflection point. Equation (I.22b) on the other hand states that the amplitude of the wavefield can be written (in the high-frequency approximation) as the ratio between the transmission loss $\mathcal{A}(\boldsymbol{\xi})$ and the geometrical-spreading factor $\mathcal{L}(\boldsymbol{\xi})$, a fact that seems also to be not very exciting.

Whereas equation (I.22a) contains nothing new indeed, equation (I.22b), however, can be used to derive an interesting relationship between the geometrical-spreading factors of the two ray segments SR_{Ref} and GR_{Ref} and the total ray $SR_{Ref}G$. For that purpose, it is convenient to introduce the "Fresnel spreading factor" (Tygel et al., 1994a)

$$\mathcal{L}_F(\boldsymbol{\xi}) \;=\; \frac{\mathcal{O}_{KH}(\boldsymbol{\xi}, \boldsymbol{\eta}_{Ref})}{|\det(\underset{\sim}{\boldsymbol{H}}_F(\boldsymbol{\xi})|^{1/2}} \; \exp\left\{ i\frac{\pi}{2}[1 - \mathrm{Sgn}(\underset{\sim}{\boldsymbol{H}}_F(\boldsymbol{\xi}))/2] \right\} \;, \tag{I.23}$$

as well as the notations

$$\mathcal{G}_0(S,R) \;=\; \mathcal{G}_0^S(\boldsymbol{\xi},\boldsymbol{\eta}) \;=\; \frac{\mathcal{A}_S(\boldsymbol{\xi},\boldsymbol{\eta})}{\mathcal{L}_S(\boldsymbol{\xi},\boldsymbol{\eta})} \tag{I.24a}$$

and

$$\mathcal{G}_0(G,R) \;=\; \mathcal{G}_0^G(\boldsymbol{\xi},\boldsymbol{\eta}) \;=\; \frac{\mathcal{A}_G(\boldsymbol{\xi},\boldsymbol{\eta})}{\mathcal{L}_G(\boldsymbol{\xi},\boldsymbol{\eta})} \;, \tag{I.24b}$$

in which $\mathcal{G}_0^S(\boldsymbol{\xi},\boldsymbol{\eta})$ represents the amplitude factor of the Green's function for the ray segment connecting $S(\boldsymbol{\xi})$ to $R(\boldsymbol{\eta})$ *after* reflection at R. Analogously, $\mathcal{A}_S(\boldsymbol{\xi},\boldsymbol{\eta})$ and $\mathcal{L}_S(\boldsymbol{\xi},\boldsymbol{\eta})$ denote the amplitude loss (due to all transmissions across overburden interfaces) and the point-source geometrical-spreading factor for this ray segment SR, respectively. The quantities $\mathcal{G}_0^G(\boldsymbol{\xi},\boldsymbol{\eta})$, $\mathcal{A}_G(\boldsymbol{\xi},\boldsymbol{\eta})$, and $\mathcal{L}_G(\boldsymbol{\xi},\boldsymbol{\eta})$ pertain to the ray segment GR. For these quantities, corresponding equations to formulas (I.20) and (I.21) can be given.

From Snell's law, the obliquity factor $\mathcal{O}_{KH}$ at the specular reflection point $R_{Ref} = R(\boldsymbol{\eta}_{Ref})$ is given by

$$\mathcal{O}_{KH}(\boldsymbol{\xi},\boldsymbol{\eta}_{Ref}) \;=\; \frac{\cos\vartheta_R(\boldsymbol{\eta}_{Ref})}{v_R(\boldsymbol{\eta}_{Ref})} \;, \tag{I.25}$$

where $\vartheta_R(\boldsymbol{\eta}_{Ref})$ denotes the angle the reflected ray $SR_{Ref}G$ makes with the normal to the reflection surface Σ_R at the reflection point R_{Ref} and $v_R(\boldsymbol{\eta}_{Ref})$ is the medium velocity just above this point. Collecting equations (I.9), (I.15b), (I.23), and (I.25), we can replace the factor $\Gamma_{KH}(\boldsymbol{\xi})$ in equation (I.22b) by

$$\Gamma_{KH}(\boldsymbol{\xi}) \;=\; \mathcal{G}_0^S(\boldsymbol{\xi},\boldsymbol{\eta}_{Ref})\; \mathcal{G}_0^G(\boldsymbol{\xi},\boldsymbol{\eta}_{Ref})\; \mathcal{L}_F(\boldsymbol{\xi}) \tag{I.26}$$

We now return to equation (I.22b), first noting the obvious fact that

$$\mathcal{A}(\boldsymbol{\xi}) \;=\; f(R)\; \mathcal{A}_S(\boldsymbol{\xi},\boldsymbol{\eta}_{Ref})\; \mathcal{A}_G(\boldsymbol{\xi},\boldsymbol{\eta}_{Ref}) \;, \tag{I.27}$$

namely that the total transmission loss in amplitude (due to crossing all overburden interfaces along the whole ray path) is the product of the transmission losses along the two ray segments. Formula (I.27) can be readily induced from the equations for $\mathcal{A}_S$ and $\mathcal{A}_G$ corresponding to expressions (I.20). Together with equations (I.24), we obtain the important *decomposition* formula

$$\mathcal{L}(\boldsymbol{\xi}) \;=\; \frac{\mathcal{L}_S(\boldsymbol{\xi},\boldsymbol{\eta}_{Ref})\; \mathcal{L}_G(\boldsymbol{\xi},\boldsymbol{\eta}_{Ref})}{\mathcal{L}_F(\boldsymbol{\xi})} \;. \tag{I.28}$$

The decomposition formula (I.28) has been previously derived in different ways for acoustic waves (Goldin, 1991; Schleicher et al., 1993; Tygel et al., 1994a). For elementary elastic waves, it has recently been deduced by Ursin and Tygel (1998). Formula (I.28) explains why $\mathcal{L}_F$ is called the "Fresnel spreading factor." It accounts for the influence of the Fresnel zone at $R(\boldsymbol{\eta}_{Ref})$, described by the Fresnel matrix $\underset{\sim}{\boldsymbol{H}}_F$, on the total geometrical spreading along the complete ray SRG. Although it has not been explicitly stated there, formula (I.28) is fundamental for the theory of true-amplitude Kirchhoff prestack migration as presented in Schleicher et al. (1993).

Let us stress that all factors used in formula (I.28) have a modulus *and* a phase. Thus, formula (I.28) provides a decomposition not only for the modulus but also for the phase of the geometrical-spreading factor, which is determined by the number of caustics. In other words, knowning the number of caustics for the ray segment SR_{Ref} (assuming a point source at S) and also that for the ray segment GR_{Ref} (assuming a point source at G), the number of caustics can be determined for the total reflected ray $SR_{Ref}G$ including the influence of the reflector (assuming a point source at either S or G). The derivation given here for a reflected wave can be done in a completely parallel way for a wavefield transmitted through an interface (with the points S and G located on opposite sides of the interface). Therefore, equations (I.27) and (I.28) are also valid for the case of transmission. This fact has been used in Hubral et al. (1995) to derive a multi-segment decomposition for the geometrical-spreading factor and the number of caustics along an arbitrary ray into point-source contributions along each segment plus additional contributions from the Fresnel zones at the intersection points.

Summary and conclusions

In Chapter I of this report, we have so far only addressed a classical forward scattering problem for a reflector below a layered, laterally smoothly inhomogeneous overburden. Using the ray-principal component, a scalar description of elementary elastic waves was introduced that allows to formulate a generalized scalar Kirchhoff representation integral. This representation was shown to be approximately valid for elementary acoustic and elastic waves. The validity conditions for this approximation are the same as for classical ray theory. Using the Kirchhoff-Helmholtz approximation in this integral, a representation of the resulting Kirchhoff-Helmholtz integral (KHI) for arbitrary measurement configurations has been obtained.

In the present representation, the effects of the overburden and the reflector on the reflected wave were separated. This separation may look artificial in the forward problem, but it will become significant when studying the inversion of the KHI. By comparison of the high-frequency evaluation of the KHI to the zero-order ray-theoretical high-frequency representation of the reflected wavefield, a decomposition formula for the geometrical-spreading factor (including the number of ray caustics) was derived.

The results obtained in Chapter I of this report will their full significance in Chapter II, where we will address the inverse problem, i.e., the recovery of the reflector image and the reflection coefficients from the recorded scattered field. Though this latter problem is, of course, in principle as well-solved as the forward problem [it is in fact often based on the Generalized Radon Transform (Gubernatis et al., 1977a; Gubernatis et al., 1977b; Beylkin, 1985), and can be either mathematically (Bleistein, 1987; Miller et al., 1987) or geometrically motivated (Schleicher et al., 1993)], the relationship between both forward and inverse scattering problems in a laterally inhomogeneous environment and for arbitrary measurement configuration (i.e., not only for shot records) has, in our opinion, not been as sufficiently elaborated in wave-theoretical terms as is done here. This applies particularly to the situation when considering measurement configurations other than that of a shot record. We think that this relationship is particularly well exposed once the connection between the diffraction-stack integral (DSI) (that solves the migration/inversion problem) and the KHI (that solves the forward scattering problem) is established. In Chapter II, we attempt to provide this connection. There we will briefly review the theory of the DSI along the lines applied in this chapter to the KHI. Thereafter, we will be ready to formulate both integrals as "physically inverse" to each other.

CHAPTER II: MIGRATION/INVERSION

Introduction

In Chapter I of this report, we have dealt with one of the surface-integral solutions to the scalar wave equation (Wapenaar and Berkhout, 1993), namely the well-known Kirchhoff integral (Sommerfeld, 1964). It computes the propagation of reflected waves away from the secondary sources using the field and its normal derivative on a closed boundary encompassing the observation point. Although mathematically not consistent and therefore obviously strictly not correct, it is often useful to approximate the field at the reflector by the so-called "Kirchhoff-Helmholtz boundary conditions" (Sommerfeld, 1964). These replace the total field on the closed boundary by the incident field (or by the specularly reflected field in case of reflected waves) on the illuminated portion of the boundary. Inserting these boundary conditions into the Kirchhoff integral provides in fact a high-frequency approximation, referred to as the "Kirchhoff-Helmholtz approximation." The resulting integral (which is very frequently used for forward seismic modeling) is briefly called the "Kirchhoff-Helmholtz integral (KHI)." In Chapter I, this integral was explicitly formulated for a smooth reflector below a layered, smoothly varying overburden (in which ray theory applies) and arbitrary seismic measurement configurations (i.e., not only a shot record).

In contrast to their usefulness in forward modeling problems, neither the original Kirchhoff integral nor the KHI is suited for solving the inverse problem, because neither of them is capable of backward propagating the wavefield in direction towards the secondary sources. The problem is conventionally circumvented by replacing retarded Green's functions in the integral by advanced ones, thus forward propagating imploding waves instead of backward propagating the true exploding ones (Porter, 1970; Bojarski, 1982). In this way, one can achieve to image the reflector and/or find the interface reflection coefficients. A recent approach to image reflected waves is based on the geometrically motivated (Hagedoorn, 1954) diffraction stack, where the wavefield, recorded in an arbitrary measurement configuration, is summed up along *diffraction traveltime surfaces* and the obtained values are assigned to the corresponding *diffraction points.* The mathematical formulation of this procedure in the high-frequency approximation (see, e.g., Schleicher et al., 1993) leads to the weighted "diffraction-stack integral (DSI)." The result of applying the DSI to seismic data is the image of the subsurface reflector giving a measure of the reflection coefficient at any reflector location.

In this Chapter II, we will address the inverse problem, i.e., the recovery of the reflector image and the determination of the reflection coefficients from the recorded scattered field. Though this inverse problem, of course, has been as well-solved as the forward problem, dealt with in Chapter I (Bleistein, 1987; Miller et al., 1987; Schleicher et al., 1993), the relationship between both forward and inverse scattering problems has, in our opinion, so far not been as sufficiently elaborated in wave-theoretical terms as is done here. This relationship is particularly well exposed once the connection between the DSI (that solves the migration/inversion problem) and the KHI (that solves the forward modeling problem) is established. It is our aim to establish this connection. We will start by briefly reviewing the theory of the DSI along the lines as done in Chapter I with the KHI. Thereafter, we will be ready to formulate the desired relationship between both integrals in physical terms.

Our investigation will provide a physical meaning to the heuristic ansatz chosen for the DSI in Schleicher et al. (1993). In this way, its relationship to the KHI will be revealed. As shown below, both integrals give rise to closely related transform operations. Our objective here is no more than to show that the DSI and the KHI are closely related operations, in the sense that the DSI recovers the information that is input to the KHI. This fact might appear to be intuitively obvious but, in our opinion, still requires a sound mathematical analysis (that involves the application of the stationary-phase method) to demonstrate the relationship in an asymptotic sense.

Our analysis will lead us to the following physical interpretation of both integrals, which will be quantified below. The KHI is understood as the superposition of Huygens elementary waves that explode along the reflector. Their source strengths are proportional to local plane-wave reflection coefficients. The DSI on the other hand is the operation that recovers the strength of the Huygens sources along the reflector. Each Huygens source would, if exploding on its own, generate seismic energy that constructively interferes along a *diffraction traveltime surface* in the seismic data. The weighted stacking of the seismic trace amplitudes along this surface by the DSI is nothing more than

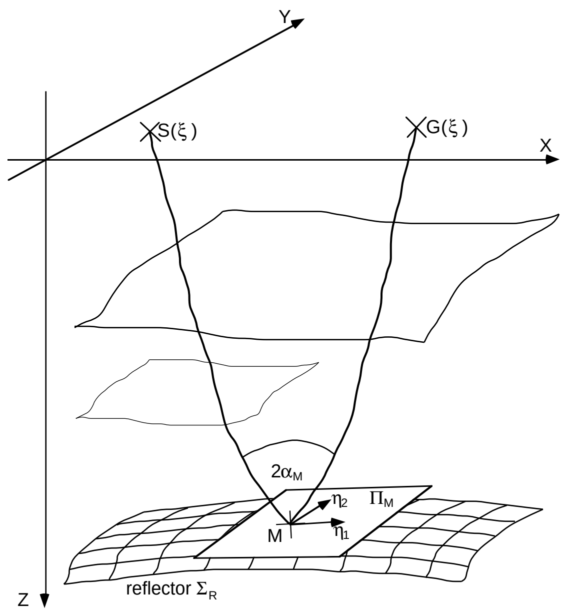

FIG. II.1. Laterally inhomogeneous Earth model with smoothly curved interfaces. Also indicated is a ray that joins the source point S via an arbitrary medium point M, here chosen to lie on the reflector Σ_R (hatched surface), to the corresponding receiver at point G. The plane Π_M is the tangent plane to the reflector at M. Its normal vector halfs the angle $2\alpha_M$ between the source ray segment SM and the receiver ray segment MG.

summing up all contributions that come from this particular Huygens wave center. In this way, the DSI can be though of as a "physical inverse" to the KHI. Note that for the following demonstration that KHI and DSI are physically inverses to each other in the sense described above, we will assume the reflector Σ_R (Figure II.1) to be specified in both operations. We then only need to consider points on Σ_R. However, the DSI can also be interpreted as a physical inverse to the KHI in an even broader sense as also the reflector location, that is an "input" to the KHI, can be recovered (Schleicher et al., 1993).

Diffraction-stack integral

A general imaging approach which allows for arbitrary measurement configurations is based on the weighted diffraction-stack integral (DSI) (Bleistein, 1987; Schleicher et al., 1993), applied to the recorded seismic traces along diffraction-time surfaces (Huygens surfaces) that are constructed with the help of a laterally inhomogeneous macro-velocity model. Based on asymptotic high-frequency evaluations, one can show that the DSI provides not only the reflector location (imaging), but also amplitudes on the reflector that are free of geometrical-spreading losses. Appropriate weight functions need only be specified. They depend on the macro-velocity model and on the measurement configuration.

For a given weight or kernel function $K_{DS}(\boldsymbol{\xi}, M)$ determined by a fixed point M within the medium (see Figure II.1) and all source-receiver pairs $(S(\boldsymbol{\xi}), G(\boldsymbol{\xi}))$, with $\boldsymbol{\xi}$ defined in the aperture set A, the DSI can be written as (1993)]

$$d(M,t) \;=\; \frac{-1}{2\pi} \iint_A d^2\boldsymbol{\xi}\; K_{DS}(\boldsymbol{\xi}, M)\; \frac{\partial D}{\partial t}(\boldsymbol{\xi}, t + \tau_D(\boldsymbol{\xi}, M)) \;. \tag{II.1}$$

We now construct the plane Π_M through point M normal to $\boldsymbol{n}_M$. On that plane, we define an arbitrary 2D-Cartesian coordinate system $\boldsymbol{\eta} = (\eta_1, \eta_2)$. With this coordinate system, we recognize equation (II.1) as an integral transformation that can be represented, in accordance to equation (I.14) for the Kirchhoff-Helmholtz integral, in the symbolic form

$$d(\boldsymbol{\eta}, t) \;=\; I_{DS}[D(\xi, t)](\boldsymbol{\eta}, t) \;. \tag{II.2}$$

The above integral represents a weighted stack (i.e., a weighted summation) over all analytic data traces $D(\boldsymbol{\xi}, t)$. This stack is performed along the diffraction-time surfaces

$$\tau \;=\; t + \tau_D(\boldsymbol{\xi}, M) = t + \tau(S(\boldsymbol{\xi}), M) + \tau(G(\boldsymbol{\xi}), M), \tag{II.3}$$

where $\boldsymbol{\xi}$ varies over the aperture set A. This is the reason, why integral (II.1) is called a "diffraction stack." In equation (II.3), $\tau(S(\boldsymbol{\xi}), M)$ and $\tau(G(\boldsymbol{\xi}), M)$ designate the traveltimes along the rays SM and MG, respectively. The value $d(M, t = 0)$ is the analytic migration output that is allocated to point M. In case of real-valued reflection coefficients, its real part is sufficient. The function $K_{DS}(\boldsymbol{\xi}, M)$ is specified as follows. Assuming the source-receiver pair $(S(\boldsymbol{\xi}), G(\boldsymbol{\xi}))$ fixed, we trace from M the rays MS and MG and consider the vector

$$\boldsymbol{n}_M \;=\; \boldsymbol{\nabla}_M[\tau(S, M) + \tau(G, M)] = \boldsymbol{\nabla}_M \tau_D(\boldsymbol{\xi}, M), \tag{II.4}$$

where $\boldsymbol{\nabla}_M$ denotes the 3D-vector gradient with respect to dislocation of M. In other words, the vector $\boldsymbol{n}_M$ is the interface normal to a (real or hypothetical) interface at which a specular reflection that follows the ray SMG takes place. In the case of a monotypical reflection (e.g., a pure P-wave reflection) at M, this vector bisects the angle between the slowness vectors of the two rays SM and GM at M, because then

$$|\boldsymbol{\nabla}_M \tau(S, M)| \;=\; |\boldsymbol{\nabla}_M \tau(G, M)| = 1/v(M) \;. \tag{II.5}$$

where $v(M)$ is the wave velocity at point M that is, in this case, the same for both ray segments.

According to Schleicher et al. (1993), the kernel $K_{DS}(\boldsymbol{\xi}, M)$ should be specified as

$$K_{DS}(\boldsymbol{\xi}, M) = \frac{\mathcal{M}(\boldsymbol{\xi},\boldsymbol{\eta})\mathcal{O}_{DS}(\boldsymbol{\xi},\boldsymbol{\eta})}{\mathcal{G}_0^S(\boldsymbol{\xi},\boldsymbol{\eta})\mathcal{G}_0^G(\boldsymbol{\xi},\boldsymbol{\eta})}, \tag{II.6}$$

where

$$\mathcal{O}_{DS}(\boldsymbol{\xi},\boldsymbol{\eta}) = \frac{v_M(\boldsymbol{\eta})}{\cos\vartheta_M(\boldsymbol{\eta})} \tag{II.7a}$$

and

$$\mathcal{M}(\boldsymbol{\xi},\boldsymbol{\eta}) = \left| \det\left(\left. \frac{\partial^2 \tau_D}{\partial\xi_i \partial\eta_j} \right|_{(\boldsymbol{\xi},\boldsymbol{\eta})} \right) \right| . \tag{II.7b}$$

The factors $\mathcal{G}_0^S(\boldsymbol{\xi},\boldsymbol{\eta})$ and $\mathcal{G}_0^G(\boldsymbol{\xi},\boldsymbol{\eta})$ are the same as explained in Chapter I.

In analogy to equation (I.19a), let us suppose that in integral (II.1) the data function $D(\boldsymbol{\xi}, t) = D(S(\boldsymbol{\xi}), G(\boldsymbol{\xi}), t)$ can be appropriately described by the zero-order ray solution of the reflection response from interface Σ_R for the pair $(S(\boldsymbol{\xi}), G(\boldsymbol{\xi}))$, namely

$$D(\boldsymbol{\xi}, t) = U_0(\boldsymbol{\xi})\; F(t - \tau_{Ref}(\boldsymbol{\xi})) , \tag{II.8}$$

with $U_0(\boldsymbol{\xi})$ given by equation (I.19b). Then, we can readily rewrite the DSI given by equation (II.1) as

$$d(\boldsymbol{\eta}, t) = \frac{-1}{2\pi} \iint_A d^2\boldsymbol{\xi}\; K_{DS}(\boldsymbol{\xi}, M)\; U_0(\boldsymbol{\xi})\; \frac{\partial}{\partial t} F(t + [\tau_D(\boldsymbol{\xi}, M) - \tau_{Ref}(\boldsymbol{\xi})]). \tag{II.9}$$

Both real and imaginary parts of the value $d(M, t = 0)$ are close to zero, if M is sufficiently away from the reflector Σ_R. For points M vertically above or below the reflector, in the near vicinity of it, $d(M, t = 0)$ is a well defined analytic pulse as a function of M (Tygel et al., 1994b). Consequently formula (II.9) does not only describe the depth-migrated image of the reflection (II.8) upon Σ_R, but it describes the whole "signal bed" (of variable thickness) to which the depth-migrated signals located along the interface Σ_R are confined. If the phase property of the source signal $F(t)$ (causal, minimum-phase, symmetric, anti-symmetric, etc.) is known, it will be possible to determine the exact reflector location Σ_R from the diffraction stack output.

In the framework of the theory presented in this work, our aim is to relate the DSI to the KHI. For that purpose, we confine in the following analysis the asymptotic evaluation of the former integral (that is done along the same lines as applied in Chapter I to the KHI) only to the case that M falls upon Σ_R.

Asymptotic evaluation of the DSI

In a similar way as we performed the asymptotic evaluation of the KHI, we can evaluate the DSI given by formula (II.9) for the case where point M lies on the reflector Σ_R, namely by setting $M = R(\boldsymbol{\eta})$. It is appropriate to rewrite equation (II.9) for this case and replace point M by the parameter vector $\boldsymbol{\eta}$. We have then

$$d(\boldsymbol{\eta}, t) = \frac{-1}{2\pi} \iint_A d^2\boldsymbol{\xi}\; K_{DS}(\boldsymbol{\xi}, \boldsymbol{\eta})\; U_0\; \frac{\partial F}{\partial t}(\boldsymbol{\xi}, t + \tau_D(\boldsymbol{\xi}, \boldsymbol{\eta})) , \tag{II.10a}$$

where

$$K_{DS}(\boldsymbol{\xi},\boldsymbol{\eta}) = \frac{\mathcal{M}(\boldsymbol{\xi},\boldsymbol{\eta})\mathcal{O}_{DS}(\boldsymbol{\xi},\boldsymbol{\eta})}{\mathcal{G}_0^S(\boldsymbol{\xi},\boldsymbol{\eta})\mathcal{G}_0^G(\boldsymbol{\xi},\boldsymbol{\eta})}, \tag{II.10b}$$

with $\mathcal{M}(\boldsymbol{\xi},\boldsymbol{\eta})$ and $\mathcal{O}_{DS}(\boldsymbol{\xi},\boldsymbol{\eta})$ given by equations (II.7). Note that in the DSI only $\boldsymbol{\xi}$ varies whereas $\boldsymbol{\eta}$ remains a fixed parameter.

The asymptotic evaluation of the DSI in the form given by equation (II.10a) at point $R = R(\boldsymbol{\eta})$ on the reflector Σ_R can, as in the case of the KHI, be obtained using the stationary-phase method in the frequency domain and, returning afterwards to the time domain. We find,

$$\begin{aligned} I_{DS}[D(\xi,t)](\boldsymbol{\eta},t) &= d(\boldsymbol{\eta},t) \\ &\simeq \Gamma_{DS}(\boldsymbol{\eta})\; U_0(\boldsymbol{\xi}_{Ref}(\boldsymbol{\eta}))\; F(t), \end{aligned} \tag{II.11a}$$

where

$$\Gamma_{DS}(\boldsymbol{\eta}) = \frac{K_{DS}(\boldsymbol{\xi}_{Ref}(\boldsymbol{\eta}),\boldsymbol{\eta})\;\exp\left\{-i\frac{\pi}{2}[1-\mathrm{Sgn}(\underset{\sim}{\boldsymbol{A}}_{Ref}(\boldsymbol{\eta}))/2]\right\}}{|\det(\underset{\sim}{\boldsymbol{A}}_{Ref}(\boldsymbol{\eta}))|^{1/2}} \tag{II.11b}$$

in which $\underset{\sim}{\boldsymbol{A}}_{Ref}(\boldsymbol{\eta})$ denotes the Hessian matrix

$$\underset{\sim}{\boldsymbol{A}}_{Ref}(\boldsymbol{\eta}) = \left(\frac{\partial^2[\tau_D(\boldsymbol{\xi},\boldsymbol{\eta})-\tau_{Ref}(\boldsymbol{\xi})]}{\partial\xi_i\partial\xi_j}\right)\Bigg|_{(\boldsymbol{\xi}_{Ref}(\boldsymbol{\eta}),\boldsymbol{\eta})} . \tag{II.11c}$$

The expression $\mathrm{Sgn}(\underset{\sim}{\boldsymbol{A}}_{Ref})$ denotes the signature of the matrix $\underset{\sim}{\boldsymbol{A}}_{Ref}$, which is assumed to be non-singular. The vector $\boldsymbol{\xi}_{Ref}(\boldsymbol{\eta})$ signifies the stationary phase point of integral (II.10a), i.e, the point where

$$\frac{\partial(\tau_D(\boldsymbol{\xi},\boldsymbol{\eta})-\tau_{Ref}(\boldsymbol{\xi}))}{\partial\xi_i}\Bigg|_{\boldsymbol{\xi}_{Ref}} = 0 \qquad \text{for } i=1,2\;. \tag{II.12}$$

It defines that particular source-receiver pair $(S(\boldsymbol{\xi}_{Ref}),G(\boldsymbol{\xi}_{Ref}))$, for which the two segments SR and RG form a total ray SRG that is specularly reflected at R. The function $\boldsymbol{\xi}_{Ref} = \boldsymbol{\xi}_{Ref}(\boldsymbol{\eta})$ determined by equation (II.12) is the inverse function to $\boldsymbol{\eta}_{Ref} = \boldsymbol{\eta}_{Ref}(\boldsymbol{\xi})$ that results from the asymptotic evaluation of the KHI. It is represented by equation (I.18). More explicitely, we have for each pair of functions $\boldsymbol{\xi}_{Ref} = \boldsymbol{\xi}_{Ref}(\boldsymbol{\eta})$ and $\boldsymbol{\eta}_{Ref} = \boldsymbol{\eta}_{Ref}(\boldsymbol{\xi})$ with $\boldsymbol{\xi}$ and $\boldsymbol{\eta}$ in their respective domains of definition the relationships

$$\boldsymbol{\xi}_{Ref}(\boldsymbol{\eta}_{Ref}(\boldsymbol{\xi})) = \boldsymbol{\xi} \qquad \text{and} \qquad \boldsymbol{\eta}_{Ref}(\boldsymbol{\xi}_{Ref}(\boldsymbol{\eta})) = \boldsymbol{\eta}\;. \tag{II.13}$$

As shown in Hubral et al. (1992), the matrix $\underset{\sim}{\boldsymbol{A}}_{Ref}(\boldsymbol{\eta})$ can be decomposed as

$$\underset{\sim}{\boldsymbol{A}}_{Ref}(\boldsymbol{\eta}) = \underset{\sim}{\boldsymbol{\Lambda}}^T_{Ref}(\boldsymbol{\eta})\,\underset{\sim}{\boldsymbol{H}}^{-1}_F(\boldsymbol{\xi}_{Ref}(\boldsymbol{\eta}))\underset{\sim}{\boldsymbol{\Lambda}}_{Ref}(\boldsymbol{\eta}), \tag{II.14a}$$

where $\underset{\sim}{\boldsymbol{\Lambda}}_{Ref}(\boldsymbol{\eta})$ denotes the second-order mixed-derivative matrix

$$\underset{\sim}{\boldsymbol{\Lambda}}_{Ref}(\boldsymbol{\eta}) = \left(\frac{\partial^2\tau_D(\boldsymbol{\xi},\boldsymbol{\eta})}{\partial\xi_i\partial\eta_j}\right)\Bigg|_{(\boldsymbol{\xi}_{Ref}(\boldsymbol{\eta}),\boldsymbol{\eta})} \tag{II.14b}$$

and $\underset{\sim}{\boldsymbol{H}}_F(\boldsymbol{\xi})$ is the so-called Fresnel-zone matrix given by equation (I.16). The superscript ^{T} indicates the transpose, while the superscript $^{-1}$ denotes the inverse. From a comparison of equations (II.14a) and (II.7b) follows readily that

$$|\det(\underset{\sim}{\boldsymbol{A}}_{Ref}(\boldsymbol{\eta})|^{1/2} = \frac{|\det(\underset{\sim}{\boldsymbol{\Lambda}}_{Ref}(\boldsymbol{\eta})|}{|\det(\underset{\sim}{\boldsymbol{H}}_F(\boldsymbol{\xi}_{Ref}(\boldsymbol{\eta}))|^{1/2}} = \frac{\mathcal{M}(\boldsymbol{\xi}_{Ref}(\boldsymbol{\eta}),\boldsymbol{\eta})}{|\det(\underset{\sim}{\boldsymbol{H}}_F(\boldsymbol{\xi}_{Ref}(\boldsymbol{\eta}))|^{1/2}} \tag{II.15a}$$

and

$$\mathrm{Sgn}(\underset{\sim}{\boldsymbol{A}}_{Ref}(\boldsymbol{\eta})) = \mathrm{Sgn}(\underset{\sim}{\boldsymbol{H}}_{Ref}(\boldsymbol{\xi}_{Ref}(\boldsymbol{\eta}))). \tag{II.15b}$$

Using equation (I.23), we obtain

$$\Gamma_{DS}(\boldsymbol{\eta}) \;=\; \frac{K_{DS}(\boldsymbol{\xi}_{Ref}(\boldsymbol{\eta}),\boldsymbol{\eta})}{\mathcal{O}_{KH}(\boldsymbol{\xi}_{Ref})\;\mathcal{L}_F(\boldsymbol{\xi}_{Ref}(\boldsymbol{\eta}))\;\mathcal{M}(\boldsymbol{\xi}_{Ref}(\boldsymbol{\eta}),\boldsymbol{\eta})}\;. \tag{II.16}$$

Further recognizing from comparison of equations (I.25) and (II.7a) that

$$\mathcal{O}_{DS}(\boldsymbol{\xi}_{Ref}) \;=\; 1/\mathcal{O}_{KH}(\boldsymbol{\eta}_{Ref}) \;=\; \frac{v_R}{\cos\vartheta_R} \tag{II.17}$$

we end up with the result

$$\Gamma_{DS}(\boldsymbol{\eta}) \;=\; 1/\mathcal{L}_F(\boldsymbol{\xi}_{Ref}(\boldsymbol{\eta}))\;\mathcal{G}_0^S(\boldsymbol{\xi}_{Ref}(\boldsymbol{\eta}),\boldsymbol{\eta}))\;\mathcal{G}_0^G(\boldsymbol{\xi}_{Ref}(\boldsymbol{\eta}),\boldsymbol{\eta})\;. \tag{II.18}$$

Comparing equations (II.18) and (I.26), we observe that $\Gamma_{DS} = 1/\Gamma_{KH}$. Upon the use of this observation together with equations (I.19b), (I.22b) and (II.13), expression (II.11a) simplifies to

$$d(\boldsymbol{\eta},t) \;=\; u(\boldsymbol{\eta},t)\;, \tag{II.19}$$

where $u(\boldsymbol{\eta},t)$ is given by equation (I.12). Result (II.19) states that the "output" of the DSI at a refection point is exactly the "input" for the KHI. Using the symbolic notations of equations (I.14) and (II.2), we may write

$$\begin{aligned} I_{DS}[I_{KH}[R_c(\boldsymbol{\eta}')F(t)](\xi,t)](\boldsymbol{\eta},t) \;&=\; I_{DS}[U_0(\boldsymbol{\xi})F(t-\tau_Ref(\xi))](\boldsymbol{\eta},t) \\ &=\; R_c(\boldsymbol{\eta}')F(t)\;, \end{aligned} \tag{II.20}$$

i.e., the DSI can be interpreted as an (asymptotic) inverse to the KHI. This fact can be physically interpreted as follows. In the same way as the KHI superposes the contributions of all Huygens sources (originating along the reflector Σ_R) to determine the reflection response at the receivers, the DSI decomposes the reflection response in order to reconstruct the source strength of a Huygens source at Σ_R. Consequently, we may say that a diffraction stack sums up all contributions in the recorded data that pertain to one particular Huygens secondary source on Σ_R (Figure II.2).

From this observation, we conclude that the DSI is the (high-frequency asymptotic) physical inverse process to the KHI in the following sense. The KHI maps the reflector attributes onto the seismic reflection distributed along the reflection-time surface (in the record domain), i.e., it constructs the seismic reflection from Σ_R by the composition of the Huygens secondary-sources contributions. The DSI, on the other hand, transforms the attributes of this reflection back into the depth domain and reconstructs in this way the amplitude values (reflection coefficients) on the reflector Σ_R by decomposing the seismic reflection into its secondary-source contributions. Both transformations are not only kinematically but also dynamically correct.

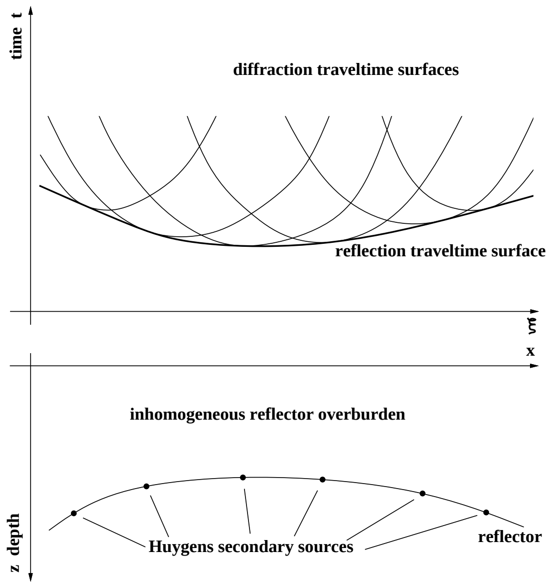

FIG. II.2. Physical interpretation of the diffraction-stack integral: Summation of all seismic amplitudes distributed in the seismic section along a diffraction traveltime surface means extracting the contributions of exactly one Huygens secondary source. Thus, if the summation is done with suitable weights, the stack will lead to a dynamically correct reconstruction of that particular Hugens source.

The asymptotic results obtained above could also be derived by application of the four-dimensional stationary-phase method to evaluate the combined integrals. This is obtained by inserting the KHI into the DSI or vice versa, which results in four-dimensional integrals (see Bleistein, 1987) which are then evaluated with the appropriate four-dimensional stationary-phase method. This approach has been used by Bleistein (1987) in the context of inverting reflector attributes by the diffraction-stack migration with the Beylkin determinant (Beylkin, 1985) as the weight function.

CONCLUSIONS

Kirchhoff inversion of data acquired in the shot-record configuration can be achieved using physical arguments, leading to back propagation together with the imaging principle (Claerbout, 1971; Schneider, 1978). For other acquisition geometries, diffraction-stack (or Kirchhoff) migration is only based on either purely geometrical considerations (Hagedoorn, 1954; Rockwell, 1971; Schleicher et al., 1993), or on mathematical ones like the Generalized Radon Transform (Beylkin, 1985; Miller et al., 1987; Bleistein, 1987). In this report, we have tried to provide a physical explanation why diffraction stack works for arbitrary measurement configurations. We have shown that the Kirchhoff-Helmholtz integral (KHI) that is widely used in forward seismic modeling to calculate the shot-record wavefield response from a given reflector and the Kirchhoff-migration integral or diffraction-stack integral (DSI) are closely related. Both integrals are specified for arbitrary measurement configurations and a laterally inhomogeneous overburden above a smooth reflector. The KHI superposes the contributions of all Huygens secondary sources located along the reflector Σ_R, to result in the reflected wavefield recorded at the receivers $G(\boldsymbol{\xi})$. The DSI, on the other hand, extracts from the recorded wavefield at all points $G(\boldsymbol{\xi})$ the Huygens source contributions to the scattered wave field and allocates their amplitudes to points on the reflecting interface. Physically spoken, the DSI represents a natural (physical) inverse to the KHI. The integral pair provides a proper theoretical understanding for the diffraction-stack migration operation and helps to physically interpret this migration procedure (often only based on either purely geometrical considerations or on mathematical ones like the Generalized Radon Transform) in terms of dynamically correct Huygens wavefield contributions. Further investigations should be carried out to examine the relationship between both integrals also for low frequencies.

The studied integral pair provides a very general and useful interpretation for transforming wavefield contributions from a known reflecting interface Σ_R either from the time domain (record domain) to the depth domain (image domain) or vice versa. Into each integral enters a macro-velocity model and a certain measurement configuration. However, we have to point out that the Kirchhoff-Helmholtz pair presented in this work is not a suitable pair to be employed for seismic imaging. With the DSI, one can image an unknown reflection event from the time domain into its image distributed along a previously unknown reflector Σ_R in the depth domain. The KHI, however, cannot transform the unknown depth image of the reflector back into the reflection event, because the knowledge of Σ_R is required in the KHI in order to perform the integration along it. Consequently, an interpretation of the migration result obtained from the DSI is necessary before applying the KHI again. This fact leads to the conclusion that the DSI is not a complete asymptotic inverse to the KHI. In fact, the true asymptotic inverse integral to the DSI is the recently establish isochrone-stack demigration integral. Details on this integral pair can be found in Hubral et al. (1996) and Tygel et al. (1996).

Acknowledgments

The research of this report has been supported in part by the sponsors of the WIT Consortium, the Brazilian National Council of Technology and Development (CNPq – Pronex), the State Research Foundation of São Paulo (FAPESP), and the Alexander von Humboldt foundation.

References

Aki, K., and Richards, P.G., 1980, Quantitative seismology – vol. 1: Theory and methods, W.H. Freeman.

Berkhout, A.J., 1985, Seismic migration – imaging of acoustic energy by wave field extrapolation. Part A: Theoretical aspects, Elsevier.

Beylkin, G., 1985, Imaging of discontinuities in the inverse scattering problem by inversion of a generalized Radon transform: J. Math. Phys., **26**, 99–108.

Bleistein, N., 1984, Mathematics of wave phenomena, Academic Press.

Bleistein, N., 1987, On the imaging of reflectors in the earth: Geophysics, **52**, 931–942.

Bojarski, N.N., 1982, A survey of the near-field far-field inverse scattering inverse source integral equation: IEEE Trans. Ant. Prop., **AP-30**, 975–979.

Born, M., and Wolf, E., 1987, Principles of optics, 6th edition, Pergamon Press, reprint.

Červený, V., 1987, Ray methods for three-dimensional seismic modelling, Norwegian Institute for Technology: Petroleum Industry Course.

Chapman, C.H., 1978, A new method for computing synthetic seismograms: Geophys. J. Roy. Astr. Soc., **54**, 481–518.

Claerbout, J.F., 1971, Toward a unified theory of reflector mapping: Geophysics, **36**, 467–481.

Docherty, P., 1991, A brief comparison of some Kirchhoff integral formulas for migration: Geophysics, **56**, 1164–1169.

Frazer, L.N., and Sen, M.K., 1985, Kirchhoff-Helmholtz reflection seismograms in a laterally inhomogeneous multi-layered elastic medium – I. Theory: Geophys. J. Roy. Astr. Soc., **80**, 121–147.

Goldin, S.V., 1991, Decomposition of geometrical approximation of a reflected wave, *in* Soviet geology and geophysics, Allerton Press, **32**, no. 7, 110–119.

Gubernatis, J.E., Domany, E., and Krumhansl, J.A., 1977a, Formal aspects of the theory of the scattering of ultrasound by flaws in elastic materials: J. Appl. Phys., **48**, 2804–2811.

Gubernatis, J.E., Domany, E., Krumhansl, J.A., and Huberman, M., 1977b, The Born approximation in the theory of the scattering of elastic waves by flaws: J. Appl. Phys., **48**, 2812–2819.

Haddon, R.A.W., and Buchen, P.W., 1981, Use of Kirchhoff's formula for body wave calculations in the earth: Geophys. J. Roy. Astr. Soc., **67**, 587–598.

Hagedoorn, J.G., 1954, A process of seismic reflection interpretation: Geophys. Prosp., **2**, 85–127.

Hubral, P., Schleicher, J., and Tygel, M., 1992, Three-dimensional paraxial ray properties – Part II. Applications: J. Seis. Expl., **1**, 347–362.

Hubral, P., Schleicher, J., and Tygel, M., 1996, A unified approach to 3-D seismic reflection imaging – Part I: Basic concepts: Geophysics, **61**, 742–758.

Hubral, P., Tygel, M., and Schleicher, J., 1995, Geometrical-spreading and ray-caustic decomposition of elementary seismic waves: Geophysics, **60**, 1195–1202.

Langenberg, K.J., 1986, Applied inverse problems for acoustic, electromagnetic, and elastic wave scattering, *in* Sabatier, P.C., Ed., Basic methods in tomography and inverse problems, Adam Hilger: Malvern Physics Series.

Miller, D., Oristaglio, M., and Beylkin, G., 1987, A new slant on seismic imaging: Migration and integral geometry: Geophysics, **52**, 943–964.

Newman, P., 1973, Divergence effects in a layered earth: Geophysics, **38**, 481–488.

Porter, R.P., 1970, Diffraction-limited scalar image formation with holograms of arbitrary shape: J. Acoust. Soc. Am., **60**, 1051–1059.

Rockwell, D.W., 1971, Migration stack aids interpretation: Oil and Gas Journal, **69**, 202–218.

Schleicher, J., Tygel, M., and Hubral, P., 1993, 3-D true-amplitude finite-offset migration: Geophysics, **58**, 1112–1126.

Schneider, W.A., 1978, Integral formulation for migration in two and three dimensions: Geophysics, **43**, 49–76.

Sommerfeld, A., 1964, Optics, Academic Press: Lectures on Theoretical Physics, **IV**.

Tygel, M., Schleicher, J., and Hubral, P., 1994a, Kirchhoff-Helmholtz theory in modelling and migration: J. Seis. Expl., **3**, 203–214.

Tygel, M., Schleicher, J., and Hubral, P., 1994b, Pulse distortion in depth migration: Geophysics, **59**, 1561–1569.

Tygel, M., Schleicher, J., and Hubral, P., 1996, A unified approach to 3-D seismic reflection imaging – Part II: Theory: Geophysics, **61**, 759–775.

Ursin, B., 1990, Offset-dependent geometrical spreading in a layered medium: Geophysics, **55**, 492–496.

Ursin, B., and Tygel, M., 1998, Reciprocal volume and surface scattering integrals for anisotropic elastic media: Wave Motion, **26**, 31–42.

Wapenaar, C.P.A., 1993, Kirchhoff-Helmholtz downward extrapolation in a layered medium with curved interfaces: Geophys. J. Internat., **115**, 445–455.

Wapenaar, C.P.A., and Berkhout, A.J., 1993, Representation of seismic reflection data – Part I: State of affairs: J. Seis. Expl., **2**, 123–131.

APPENDIX A

A scalar wave equation for elastic elementary waves

The homogeneous scalar Helmholtz equation for acoustic waves in inhomogeneous media reads (Aki and Richards, 1980)

$$\boldsymbol{\nabla}\cdot\left(\frac{1}{\rho}\boldsymbol{\nabla}\mathcal{G}(\hat{\boldsymbol{r}},\omega;\hat{\boldsymbol{r}}_S)\right)+\frac{\omega^2}{k}\mathcal{G}(\hat{\boldsymbol{r}},\omega;\hat{\boldsymbol{r}}_S)=0\;, \tag{A-1}$$

where $\mathcal{G}(\hat{\boldsymbol{r}},\omega;\hat{\boldsymbol{r}}_S)$ is the pressure, ρ is the density of the medium, and k is the bulk modulus. In high-frequency approximation, using the ansatz

$$\mathcal{G}(\hat{\boldsymbol{r}},\omega;\hat{\boldsymbol{r}}_S)=A(\hat{\boldsymbol{r}},\hat{\boldsymbol{r}}^s)\exp\{i\omega(t-\tau(\hat{\boldsymbol{r}})\}\;, \tag{A-2}$$

equation (A-1) is known to be equivalent to the system of nonlinear first-order equations consisting of the eikonal equation

$$(\boldsymbol{\nabla}\tau)^2=\frac{1}{c^2}\;,\qquad c^2=\frac{k}{\rho} \tag{A-3a}$$

and the transport equation

$$\boldsymbol{\nabla}\cdot(\frac{A^2}{\rho}\boldsymbol{\nabla}\tau)=0\;. \tag{A-3b}$$

On the other hand, the homogeneous isotropic elastic wave equation reads (Červený, 1987)

$$\rho\omega^2\check{\mathcal{G}}_{in}(\hat{\boldsymbol{r}},\omega;\hat{\boldsymbol{r}}_S)+\left(\lambda\check{\mathcal{G}}_{jn,j}(\hat{\boldsymbol{r}},\omega;\hat{\boldsymbol{r}}_S)\right)_{,i}+\left(\mu(\check{\mathcal{G}}_{jn,i}(\hat{\boldsymbol{r}},\omega;\hat{\boldsymbol{r}}_S)+\check{\mathcal{G}}_{in,j}(\hat{\boldsymbol{r}},\omega;\hat{\boldsymbol{r}}_S))\right)_{,j}=0\;, \tag{A-4}$$

where λ and μ are the Lamé parameters and δ_{ij} is the Kronecker symbol. An index following a comma means a derivative with respect to the corresponding Cartesian coordinate. The ray ansatz for the green's function of an elementary elastic wave is then (Chapman, 1978; Červený, 1987)

$$\check{\mathcal{G}}_{ij}(\hat{\boldsymbol{r}},\omega;\hat{\boldsymbol{r}}_S)=h_i(\hat{\boldsymbol{r}})\mathcal{G}(\hat{\boldsymbol{r}},\omega;\hat{\boldsymbol{r}}_S)h_j(\hat{\boldsymbol{r}}^s)\;, \tag{A-5}$$

where $\mathcal{G}(\hat{\boldsymbol{r}},\omega;\hat{\boldsymbol{r}}_S)$ denotes the principal component of the displacement and h_i is the ith coordinate of the polarization vector. The factor $\mathcal{G}(\hat{\boldsymbol{r}},\omega;\hat{\boldsymbol{r}}_S)$ can again be represented in the form of equation (A-2). Inserting this ansatz into equation (A-4), we have in the same zero-order ray approximation for the *scalar* principal components of the elastic wavefield, i.e., the elementary P- and S-waves, corresponding eikonal and transport equations. The eikonal equation reads in this case (Červený, 1987)

$$(\boldsymbol{\nabla}\tau)^2=\frac{1}{v^2}\;, \tag{A-6a}$$

where v is the wave velocity of the considered elementary P- or S-wave, respectively, i.e., $v=\sqrt{(\lambda+2\mu)/\rho}$ for an elementary P-wave or $v=\sqrt{\mu/\rho}$ for an elementary S-wave. The transport equation is correspondingly given by

$$\boldsymbol{\nabla}\cdot(\rho v^2A^2\boldsymbol{\nabla}\tau)=0\;, \tag{A-6b}$$

where we have used the known expressions for the polarization vector $\boldsymbol{h}(\hat{\boldsymbol{r}})$ for P- and S-waves at the observation point $\hat{\boldsymbol{r}}$.

For a P-wave, $\boldsymbol{h}(\hat{\boldsymbol{r}})$ is parallel to the propagation direction and thus given by

$$\boldsymbol{h}(\hat{\boldsymbol{r}}) = v\boldsymbol{\nabla}\tau \ . \tag{A-7a}$$

For an S-wave, we have the slightly more complicated expression

$$\boldsymbol{h}(\hat{\boldsymbol{r}}) = v\frac{B\boldsymbol{e}_1 + C\boldsymbol{e}_2}{A^2} \ , \tag{A-7b}$$

where $A = \sqrt{B^2 + C^2}$ is the generally complex amplitude coefficient of the principal component of the S-wave and where the unit vectors $\boldsymbol{e}_1$ and $\boldsymbol{e}_2$ form together with the unit tangential vector $\boldsymbol{t} = v\boldsymbol{\nabla}\tau$ a right-handed Cartesian coordinate system. Due to the similarity of equations (A-3a) and (A-6a) as well as (A-3b) e (A-6b), it is possible to find a scalar Helmholtz equation similar to (A-1) that describes the propagation of the principal components of elementary elastic P- or S-waves. The *general scalar Helmholtz equation for acoustic and elastic elementary waves* can be written in the form

$$\boldsymbol{\nabla} \cdot \Big(f(\hat{\boldsymbol{r}})\boldsymbol{\nabla} U^0(\hat{\boldsymbol{r}},\omega) \Big) + g(\hat{\boldsymbol{r}})\omega^2 U^0(\hat{\boldsymbol{r}},\omega) = 0 \ , \tag{A-8}$$

with the corresponding general eikonal and transport equations

$$(\boldsymbol{\nabla}\tau)^2 = \frac{g}{f} \ , \tag{A-9a}$$

$$\boldsymbol{\nabla} \cdot (f A^2 \boldsymbol{\nabla}\tau) = 0 \ . \tag{A-9b}$$

In these equations, we have

$$f = \frac{1}{\rho} \ , \quad g = \frac{1}{k} \qquad \text{for acoustic waves} \tag{A-10a}$$

$$f = \rho v^2 \ , \quad g = \rho \qquad \text{for elastic waves} \tag{A-10b}$$

Note that $\rho v^2 = \lambda + 2\mu$ for P-waves and $\rho v^2 = \mu$ for S-waves.

The physical meaning of $\mathcal{G}(\hat{\boldsymbol{r}},\omega;\hat{\boldsymbol{r}}_S)$ is, of course, different in the different cases. In the acoustic case it denotes pressure, and in the elastic case it stands for the principal component of the particle displacement for the considered elementary wave. Note that the above Helmholtz equation does not describe, of course, the polarization of the elastic elementary waves which, however, is known for the principal components to be parallel to the propagation direction for P-waves and perpendicular to that direction for S-waves.

We stress that the above scalar wave equation for elementary elastic waves is, of course, only valid where zero-order ray theory is valid, too. This means in particular that it does not correctly describe elastic reflection coefficients. So, one might wonder about the advantage one would gain from using this generalized equation. The point is that this scalar wave equation allows us to also set up a scalar Kirchhoff-Helmholtz integral for elementary seismic primary-reflected waves. This proposed integral representation (see Appendix B) yields a better wavefield approximation than ray theory. The results are satisfactorial for a broader range of frequencies and even diffractions can be modeled quite accurately.

APPENDIX B

Derivation of the scalar elastic Kirchhoff integral

Direct waves

Consider the situation depicted in Figure B-1. We have a region Q to which all the sources

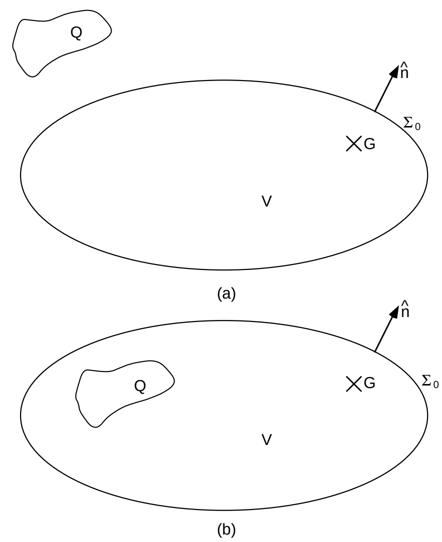

FIG. B-1. A receiver position G is located in a volume V with surface Σ_0. The sources are confined to a region Q that is (a) outside V, (b) inside V.

are confined. Also, we have a region V inside which a receiver (or observation point) G is located. In Figure B-1b, Q is a part of V, in Figure B-1a, it is not. Our aim is to compute the scalar wavefield $U^0(\hat{\boldsymbol{r}}, t)$ that will be measured at G due to the sources in Q. The wave equation that governs this problem is the scalar wave equation, which is, in the frequency domain, represented by the generalized scalar Helmholtz equation (see Appendix A)

$$\boldsymbol{\nabla} \cdot \Big(f(\hat{\boldsymbol{r}}) \boldsymbol{\nabla} U^0(\hat{\boldsymbol{r}}, \omega) \Big) + g(\hat{\boldsymbol{r}}) \omega^2 U^0(\hat{\boldsymbol{r}}, \omega) = -4\pi q(\hat{\boldsymbol{r}}, \omega) \ , \tag{B-1}$$

where $q(\hat{\boldsymbol{r}}, \omega)$ is the source function that vanishes for all $\hat{\boldsymbol{r}}$ outside Q. As we have seen in Appendix A, this Helmholtz equation may describe the propagation of as well acoustic as elementary elastic waves. For acoustic waves, we have $f = 1/\rho$ and $g = 1/k = 1/\rho c^2$, with ρ being the medium density, k its bulk modulus and c the acoustic wave velocity. For elementary elastic waves, $f = v^2$ and $g = 1$, where v is now the wave velocity of the considered elementary wave.

We know that a solution to this wave equation can be found once the Green's fuction $\mathcal{G}$ is known that fulfills the corresponding equation

$$\boldsymbol{\nabla} \cdot \left(f(\hat{\boldsymbol{r}}) \boldsymbol{\nabla} \mathcal{G}(\hat{\boldsymbol{r}}, \hat{\boldsymbol{r}}', \omega) \right) + g(\hat{\boldsymbol{r}}) \omega^2 \mathcal{G}(\hat{\boldsymbol{r}}, \hat{\boldsymbol{r}}', \omega) = -4\pi \delta(\hat{\boldsymbol{r}}, \hat{\boldsymbol{r}}') \ . \tag{B-2}$$

If equation (B-2) has been solved, a solution to equation (B-1) is readily found to be

$$U^0(\hat{\boldsymbol{r}},\omega) = \int\limits_Q dQ \;\; \mathcal{G}(\hat{\boldsymbol{r}},\hat{\boldsymbol{r}}',\omega) q(\hat{\boldsymbol{r}}',\omega) \ . \tag{B-3}$$

This can be easily checked by applying the differential operator $\boldsymbol{\nabla}\cdot(f(\hat{\boldsymbol{r}})\boldsymbol{\nabla})$ to equation (B-3) and inserting equation (B-2). We now want to find an alternative solution in terms of the wavefield at the boundary Σ_0 of V. For that purpose, we consider Gauss's divergence theorem. It states that for any arbitrary volume V with surface Σ_0 and for any arbitrary vector field $\hat{\boldsymbol{\Psi}}(\hat{\boldsymbol{r}})$ that is defined for all points $\hat{\boldsymbol{r}}$ in V and on Σ_0,

$$I_V = \int\limits_V dV \;\; \boldsymbol{\nabla}\cdot\hat{\boldsymbol{\Psi}}(\hat{\boldsymbol{r}}) = \int\limits_{\Sigma_0} d\Sigma_0 \;\; \hat{\boldsymbol{n}}\cdot\hat{\boldsymbol{\Psi}}(\hat{\boldsymbol{r}}) = I_{\Sigma_0} \ , \tag{B-4}$$

where $\hat{\boldsymbol{n}}$ is the *outward pointing* normal vector to the surface Σ_0 of V. With the particular choice

$$\hat{\boldsymbol{\Psi}} = \mathcal{G} f \boldsymbol{\nabla} U^0 - U^0 f \boldsymbol{\nabla}\mathcal{G} \ , \tag{B-5}$$

we may rewrite the left-hand-side volume integral I_V of equation (B-4) as

$$I_V = \int\limits_V dV \;\; \left[\mathcal{G}\boldsymbol{\nabla}\cdot\left(f(\hat{\boldsymbol{r}})\boldsymbol{\nabla}U^0\right) - U^0\boldsymbol{\nabla}\cdot(f(\hat{\boldsymbol{r}})\boldsymbol{\nabla}\mathcal{G})\right] \ . \tag{B-6}$$

Inserting the above wave equations (B-1) and (B-2) for the terms $\boldsymbol{\nabla}\cdot(f(\hat{\boldsymbol{r}})\boldsymbol{\nabla}U^0)$ and $\boldsymbol{\nabla}\cdot(f(\hat{\boldsymbol{r}})\boldsymbol{\nabla}\mathcal{G})$, we arrive, after some easy simplifications, at

$$I_V = -\int\limits_V dV \;\; \left[4\pi\mathcal{G}(\hat{\boldsymbol{r}},\hat{\boldsymbol{r}}',\omega)q(\hat{\boldsymbol{r}},\omega) - 4\pi U^0(\hat{\boldsymbol{r}},\omega)\delta(\hat{\boldsymbol{r}},\hat{\boldsymbol{r}}',\omega)\right] \ . \tag{B-7}$$

Let us now distinguish the two cases indicated in Figures B-1a and B-1b. (a) If Q belongs to V, the first volume integration reduces to region Q because $q(\hat{\boldsymbol{r}},\omega)$ vanishes elsewhere. The second integral containing the delta function is readily solved. The overall result is

$$I_V = -4\pi\int\limits_Q dQ \;\; \left[\mathcal{G}(\hat{\boldsymbol{r}},\hat{\boldsymbol{r}}',\omega)q(\hat{\boldsymbol{r}},\omega)\right] + 4\pi U^0(\hat{\boldsymbol{r}}',\omega) \ , \tag{B-8}$$

which vanishes due to equation (B-3). Due to the equality of the surface and volume integrals in equation (B-4), also the surface integral I_{Σ_0} on the right-hand side of that equation vanishes in this case. (b) On the other hand, if Q does not belong to V, the first integral in equation (B-7) vanishes [remember that $q(\hat{\boldsymbol{r}},\omega)$ is identical to zero outside Q], so that we arrive at

$$I_V = 4\pi U^0(\hat{\boldsymbol{r}}',\omega) \ . \tag{B-9}$$

Together with the right-hand-side of the divergence theorem (B-4), we may thus write for the wavefield $U^0(\hat{\boldsymbol{r}}_G,\omega)$ at an observation point origination from sources outside the volume V enclosed by Σ_0 G

$$U^0(\hat{\boldsymbol{r}}_G,\omega) = \frac{1}{4\pi}\int\limits_{\Sigma_0} d\Sigma_0 \;\; f(\hat{\boldsymbol{r}}) \;\; \left[\mathcal{G}(\hat{\boldsymbol{r}},\hat{\boldsymbol{r}}_G,\omega)\frac{\partial U^0(\hat{\boldsymbol{r}},\omega)}{\partial n} - U^0(\hat{\boldsymbol{r}},\omega)\frac{\partial\mathcal{G}(\hat{\boldsymbol{r}},\hat{\boldsymbol{r}}_G,\omega)}{\partial n}\right] \ , \tag{B-10}$$

where $\partial/\partial n = \hat{\boldsymbol{n}} \cdot \boldsymbol{\nabla}$ is the derivative in the direction of the surface normal. This is the famous Kirchhoff integral representation (Sommerfeld, 1964; Born and Wolf, 1987), here generally rederived for any type of scalar Helmholtz equation (B-1). We remind that $f = 1/\rho$ for acoustic waves and $f = v^2$ for elementary elastic waves.

Transmitted waves

We have seen that the wavefield at an observation point G can be computed by integral (B-10) from the values of the wavefield and its normal derivatives at a surface Σ_0 surrounding G, provided the sources of the wavefield are located outside Σ_0. The particular shape of the volume V or of the surface Σ_0 plays no role for this representation. In particular, we may extend the surface Σ_0 to a transmitting interface Σ_T, e.g., located between G and Q (see Figure B-2), and to infinity

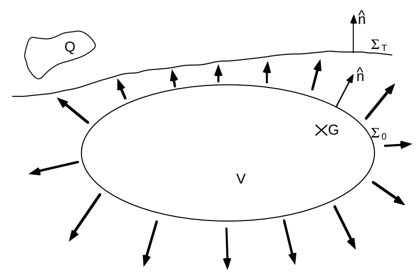

FIG. B-2. By extending the surface Σ_0 to infinity where possible and to a transmitting interface Σ_T elsewhere, the Kirchhoff integral can be reduced to an integration along Σ_T. Note that the direction of the normal vactor must be inverted.

elsewhere. The integration over infinity does not yield any contribution because the wavefield and its derivatives are required by Sommerfeld's radiation condition to vanish at infinite distance from the source. Inverting the direction of the normal vector to have it pointing *towards* G, a representation for the transmitted field $U^t(\hat{\boldsymbol{r}}_G,\omega)$ at G is thus found to be

$$U^t(\hat{\boldsymbol{r}}_G,\omega) = \frac{-1}{4\pi} \int\limits_{\Sigma_T} d\Sigma_T \;\; f(\hat{\boldsymbol{r}}) \; \left[\mathcal{G}(\hat{\boldsymbol{r}},\hat{\boldsymbol{r}}_G,\omega) \frac{\partial U^t(\hat{\boldsymbol{r}},\omega)}{\partial n} - U^t(\hat{\boldsymbol{r}},\omega) \frac{\partial \mathcal{G}(\hat{\boldsymbol{r}},\hat{\boldsymbol{r}}_G,\omega)}{\partial n} \right] , \qquad \text{(B-11)}$$

where $U^t(\hat{\boldsymbol{r}},\omega)$ inside the integral represents the wavefield at the transmitting interface Σ_T directly after transmission.

Reflected waves

Similar considerations can be used to derive a "Kirchhoff integral" for reflected waves. Consider the situation depicted in Figure B-3. We assume that the parameters of the medium are now different from the above where we have already solved the direct problem. To visualize this difference, we denote the (variable) medium parameters now by a tilde above the symbol, i.e., by $\tilde{f}$ and $\tilde{g}$. However, we assume that there exists a certain region R to which all differences are confined, i.e., $\tilde{f} \neq f$ and $\tilde{g} \neq g$ in R, but $\tilde{f} = f$ and $\tilde{g} = g$ elsewhere. The "scattering region" R is assumed to be entirely outside the volume V and the source region Q is assumed to be part of V. Our aim

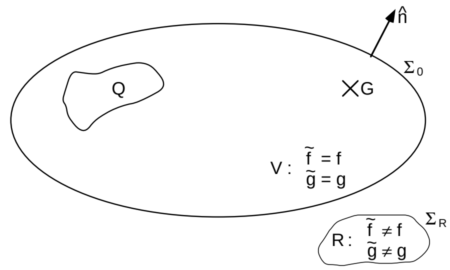

FIG. B-3. The medium parameters, $\tilde{f}$ and $\tilde{g}$, are supposed to differ from the previous ones, f and g, in region R only. The scattered wavefield due to this perturbation is to be computed at G.

is now to compute the additional contribution to the wavefield at G, i.e., the field "scattered" or "reflected" at the medium perturbations in R.

The wave equation for the total wavefield $U(\hat{\boldsymbol{r}}, \omega)$ is given correspondingly to equation (B-1) above by

$$\boldsymbol{\nabla} \cdot \left(\tilde{f}(\hat{\boldsymbol{r}}) \boldsymbol{\nabla} U(\hat{\boldsymbol{r}}, \omega) \right) + \tilde{g}(\hat{\boldsymbol{r}}) \omega^2 U(\hat{\boldsymbol{r}}, \omega) = -4\pi q(\hat{\boldsymbol{r}}, \omega) \ , \tag{B-12}$$

Subtracting now equation (B-1) from equation (B-12), and introducing the notation $U^s(\hat{\boldsymbol{r}}, \omega) = U(\hat{\boldsymbol{r}}, \omega) - U^0(\hat{\boldsymbol{r}}, \omega)$ for the scattered field, we obtain

$$\boldsymbol{\nabla} \cdot (f(\hat{\boldsymbol{r}}) \boldsymbol{\nabla} U^s(\hat{\boldsymbol{r}}, \omega)) + \omega^2 g(\hat{\boldsymbol{r}}) U^s(\hat{\boldsymbol{r}}), \omega) = -4\pi q^s(\hat{\boldsymbol{r}}, \omega) \ , \tag{B-13}$$

where

$$q^s(\hat{\boldsymbol{r}}, \omega) = \frac{1}{4\pi} \left(\boldsymbol{\nabla} \cdot [(\tilde{f} - f) \boldsymbol{\nabla} U] + \omega^2 (\tilde{g} - g) U \right) \tag{B-14}$$

describes the so-called secondary sources in the region R, i.e., the Huygens sources excited by the total field $U(\hat{\boldsymbol{r}}, \omega)$. At this point, it is worthwile to observe that $q^s(\hat{\boldsymbol{r}}, \omega) = 0$ for all $\hat{\boldsymbol{r}}$ in V, because of our assumption that all points $\hat{\boldsymbol{r}}$ where $\tilde{f} \neq f$ and $\tilde{g} \neq g$ are confined to R which was assumed to be outside V. Note that in single-scattering approximation, one would replace in equation (B-14) the total field $U(\hat{\boldsymbol{r}}, \omega)$ by the incident (direct) field $U^0(\hat{\boldsymbol{r}}, \omega)$. As equation (B-13) is just the original Helmholtz equation (B-1) with a different source term $q^s(\hat{\boldsymbol{r}}, \omega)$, its solution can be represented in form of equation (B-3) with q^s instead of q and integrating over region R instead of Q. Together with the mentioned single-scattering approximation for q^s, this is the Born approximation for the scattered wavefield.

To derive a Kirchhoff representation, we now return to Gauss's divergence theorem (B-4) using, however, a slightly different vector function $\hat{\boldsymbol{\Psi}}$, namely

$$\hat{\boldsymbol{\Psi}} = \mathcal{G} f \boldsymbol{\nabla} U - U f \boldsymbol{\nabla} \mathcal{G} \ , \tag{B-15}$$

with $\mathcal{G}$ still being a solution of Helmholtz equation (B-1), but U being now a solution of Helmholtz equation (B-12). In parallel to the above, we arrive at

$$I_V = 4\pi(U^0 + U^s) + \int_V dV \quad [-\mathcal{G}\, 4\pi q - \mathcal{G}\, 4\pi q^s] \ . \tag{B-16}$$

The first integration reduces to domain Q inside V, and thus yields $-4\pi U^0$ due to equation (B-3). The second integration vanishes because $q^s(\hat{\boldsymbol{r}}) = 0$ for all $\hat{\boldsymbol{r}}$ in V and, thus, integral (B-16) yields $I_V = 4\pi U^s$. In other words, because of equation (B-4) the result for the scattered wavefield $U^s(\hat{\boldsymbol{r}}_G, \omega)$ at G is

$$U^s(\hat{\boldsymbol{r}}_G, \omega) = \frac{1}{4\pi} \int_{\Sigma_0} d\Sigma_0 \;\; f(\hat{\boldsymbol{r}}) \;\; \left[\mathcal{G}(\hat{\boldsymbol{r}}, \hat{\boldsymbol{r}}_G, \omega) \frac{\partial U(\hat{\boldsymbol{r}}, \omega)}{\partial n} - U(\hat{\boldsymbol{r}}, \omega) \frac{\partial \mathcal{G}(\hat{\boldsymbol{r}}, \hat{\boldsymbol{r}}_G, \omega)}{\partial n} \right] \; . \qquad \text{(B-17)}$$

We now replace in the above integral U by $U^0 + U^s$ and separate the result into two surface integrals, depending on U^0 and U^s, respectively. We recognize that the integration over U^0 vanishes because Q is contained in V which leads for the direct field U^0 to equation (B-8). Thus, equation (B-17) can be recast into

$$U^s(\hat{\boldsymbol{r}}_G, \omega) = \frac{1}{4\pi} \int_{\Sigma_0} d\Sigma_0 \;\; f(\hat{\boldsymbol{r}}) \;\; \left[\mathcal{G}(\hat{\boldsymbol{r}}, \hat{\boldsymbol{r}}_G, \omega) \frac{\partial U^s(\hat{\boldsymbol{r}}, \omega)}{\partial n} - U^s(\hat{\boldsymbol{r}}, \omega) \frac{\partial \mathcal{G}(\hat{\boldsymbol{r}}, \hat{\boldsymbol{r}}_G, \omega)}{\partial n} \right] \; . \qquad \text{(B-18)}$$

Because of our assumption that all sources are confined to Q and all secondary sources (scatterers) are confied to region R, equation (B-18) is valid independently of the particular shape of Σ_0. We may thus extend it to infinity wherever possible, however in such a way that R remains outside V. At the very end of such an extension we will have essentially an integration in infinite distance from the source, where the field is required to vanish due to Sommerfeld's radiation conditions, plus a remaining integration along the surface Σ_R of R, where the surface normal is now pointing *inward*, i.e., into region R (see Figure B-4a). Changing the direction of the normal vector of this surface to pointing outward region R means changing the sign of the resulting integration. We thus finally arrive at the following expression for the reflected field $U^r(\hat{\boldsymbol{r}}_G, \omega)$ at G

$$U^r(\hat{\boldsymbol{r}}_G, \omega) = \frac{-1}{4\pi} \int_{\Sigma_R} d\Sigma_R \;\; f(\hat{\boldsymbol{r}}) \;\; \left[\mathcal{G}(\hat{\boldsymbol{r}}, \hat{\boldsymbol{r}}_G, \omega) \frac{\partial U^r(\hat{\boldsymbol{r}}, \omega)}{\partial n} - U^r(\hat{\boldsymbol{r}}, \omega) \frac{\partial \mathcal{G}(\hat{\boldsymbol{r}}, \hat{\boldsymbol{r}}_G, \omega)}{\partial n} \right] \; . \qquad \text{(B-19)}$$

This form of the Kirchhoff integral for reflected waves does not depend on whether the surface

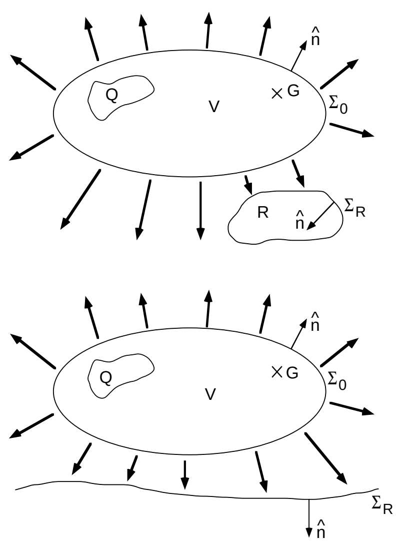

FIG. B-4. The surface Σ_0 can be extended to infinity where it does not cross the surface Σ_R. The surface Σ_R may either be (a) a closed surface or (b) a reflecting interface stretching to infinity. Note that in both cases the direction of the normal vector must be inverted.

Σ_R of R is a closed or an open surface (Figures B-4a and B-4b). Note that this integral expression describes as well acoustic as elementary elastics waves as long as the ray-theoretical approximations for $\mathcal{G}(\hat{\boldsymbol{r}}, \hat{\boldsymbol{r}}_G, \omega)$ and $U^r(\hat{\boldsymbol{r}}, \omega)$ are valid.

APPENDIX C

Kirchhoff-Helmholtz Approximation

For an explanation of the ansatz used in the Kirchhoff-Helmholtz approximation, let us first consider the simple case of a transmission (resp. reflection) of a plane wave at a planar interface betweeen to homogeneous half-spaces. Without loss of generality, we assume the interface to be horizontal and to coincide with the plane $z = 0$, where the z-axis is pointing into the lower medium (Figure C-1). Leaving the time-harmonic dependency $\exp\{i\omega t\}$ aside, a monofrequency plane wave

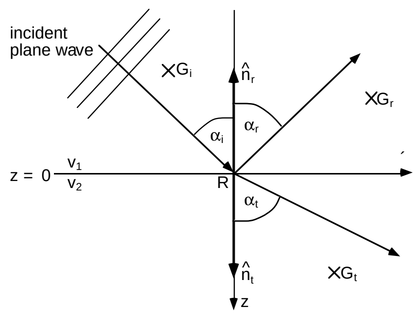

Fig. C-1. A plane wave impinges onto a planar interface located at $z = 0$.

incident from above, e.g., when passing through point G_i, is generally described by

$$U_i(\omega) \;=\; A\,\exp\left\{-i\omega\left(\eta\frac{\sin\alpha^-}{v^-}+z\frac{\cos\alpha^-}{v^-}\right)\right\}\;, \tag{C-1}$$

where A is the (constant) amplitude and v^- is the wave velocity for the incident field. In Figure C-1, $v^- = v_1$, i.e., the (constant) medium velocity above the interface. The quantity α^- is the acute angle that the propagation direction makes with the z-axis. Also, we have used the horizontal coordinate $\eta = x\cos\varphi + y\sin\varphi$, where φ is the azimuth angle within the xy-plane. The wavefield at an observation point G_t (G_r) after being transmitted (reflected) at the plane $z = 0$ is then given by

$$U_a(\omega) \;=\; C_a\,A\,\exp\left\{-i\omega\left(\eta\frac{\sin\alpha^+}{v^+}\pm z\frac{\cos\alpha^+}{v^+}\right)\right\}\;, \tag{C-2}$$

where C_a is the transmission (reflection) coefficient. Quantities that are marked with an upper index $^-$ denote parameters before incidence at the interface and those marked with $^+$ denote parameters after transmission (reflection). For instance, in Figure C-1 for transmission $v^+ = v_2$, for (monotypical) reflection $v^+ = v_1$. The index a can be t for transmission and r for reflection. The upper sign in equation (C-2) holds for transmission, the lower one for reflection.

In the Kirchhoff integral (B-10), the normal derivative of the field to be propagated at the surface Σ_0 is needed. To compute the corresponding derivatives of the above wavefields, let us first take their gradients. We find

$$\boldsymbol{\nabla} U_i \;=\; -\,i\omega\left(\cos\varphi\,\frac{\sin\alpha^-}{v^-},\sin\varphi\,\frac{\sin\alpha^-}{v^-},\,\frac{\cos\alpha^-}{v^-}\right)^T\;U_i \tag{C-3}$$

and

$$\boldsymbol{\nabla} U_a \;=\; -\,i\omega \left(\cos\varphi \,\frac{\sin\alpha^+}{v^+}, \sin\varphi\,\frac{\sin\alpha^+}{v^+}, \pm\frac{\cos\alpha^+}{v^+} \right)^T \; U_a \; . \tag{C-4}$$

To obtain the normal derivatives of the fields, one simply has to multiply the above gradients with the surface normal $\hat{\boldsymbol{n}}$ at the transmission (reflection) point. However, there are two possible definitions for the surface normal of the interface at $z = 0$. Which one is correct? In the Kirchhoff integrals (B-11) and (B-19) for the transmission and reflection case, respectively, the normal vectors are defined as outward normals on the surfaces Σ_T and Σ_R, i.e., pointing towards the respective observation point G_t or G_r. Thus, we now have to introduce different normal vectors for the reflected ($\hat{\boldsymbol{n}}_r$) and transmitted ($\hat{\boldsymbol{n}}_r$) wavefields. We must use (Figure C-1)

$$\hat{\boldsymbol{n}}_r \;=\; (0,0,1)^T \qquad \text{and} \qquad \hat{\boldsymbol{n}}_t \;=\; (0,0,-1)^T \; . \tag{C-5}$$

With these normal vectors, we arrive at

$$\hat{\boldsymbol{n}}_a \cdot \boldsymbol{\nabla} U_a \;=\; \frac{\partial U_a}{\partial n} \;=\; +\,i\omega\frac{\cos\alpha^+}{v^+}\, U_a \; , \tag{C-6}$$

where we have also taken into account that α^- and α^+ denote acute angles with the z-axis. Multplying also the incident field with these normal vectors, we have

$$\hat{\boldsymbol{n}}_a \cdot \boldsymbol{\nabla} U_i \;=\; \frac{\partial U_i}{\partial n} \;=\; \pm\,i\omega\frac{\cos\alpha^-}{v^-}\, U_i \; . \tag{C-7}$$

Note that the sign of the normal derivative of the reflected wave in equation (C-6) is *inverted* with respect to that of the incident field (C-7). This is due to the "inverted" propagation direction ("upward" instead of "downward" propagation). Although the normal derivative of the transmitted wave in expression (C-6) has the identical sign to that of the reflected wave, it has in fact the *same* sign as the corresponding normal derivative of the incident field (C-7). This is due to the reversal of the direction of the normal vector.

Let us now consider the situation at point R on the interface ($z = 0$). Comparing equations (C-1) and (C-2), we observe that

$$U_a\Big|_{z=0} \;=\; C_a\; U_i\Big|_{z=0} \tag{C-8a}$$

and inserting this into equation (C-6), we find

$$\frac{\partial U_a}{\partial n}\Big|_{z=0} \;=\; +\,i\omega\frac{\cos\alpha^+}{v^+}\; C_a\; U_i\Big|_{z=0} \; . \tag{C-8b}$$

Now it is easy to explain what is done in the Kirchhoff-Helmholtz approximation used in the Kirchhoff integral. In the Kirchhoff integral, there appear both the expressions U_a and $\partial U_a/\partial n$ at an arbitrary interface Σ_R and with an arbitrary incident field. The Kirchhoff-Helmholtz approximation now simply assumes that the equations (C-8a) and (C-8b) are also valid in this general case, i.e., at each point R on Σ_R,

$$U_a\Big|_R \;=\; C_a\; U_i\Big|_R \; , \tag{C-9a}$$

$$\frac{\partial U_a}{\partial n}\Big|_R \;=\; +\,i\omega\frac{\cos\alpha_R^+}{v_R^+}\; C_a\; U_i\Big|_R \; , \tag{C-9b}$$

where we have denoted the velocity at R *after* specular reflection by v_R^+ to indicate that this approximation may also be made in (slightly) inhomogeneous media. Physically spoken, it is assumed in this approximation that the incident wavefield locally behaves like a plane wave and that the reflector Σ_R locally acts like a planar interface at R. The amplitude variation of a non-plane wave is neglected.

Moreover, correspondingly to equation (C-9b), it is also assumed that the Green's function approximately fulfills

$$\left.\frac{\partial \mathcal{G}_a(\hat{\boldsymbol{r}}, \hat{\boldsymbol{r}}')}{\partial n}\right|_R = -i\omega \frac{\cos \alpha_R^G}{v_R^+} \left.\mathcal{G}_a\right|_R , \tag{C-10}$$

where α_R^G is the angle that the ray from R to G makes with $\hat{\boldsymbol{n}}$ ar R. This high-frequency approximation corresponds to zero-order ray-theory assumptions.

It is to be remarked that equation (C-9b) simplifies for the particular case of a *monotypical reflection* (i.e., a P-P S-S or acoustic reflection). In this case, which is usually considered in the literature, $v^- = v^+$ and $\alpha^- = \alpha^+$. Therefore, upon the use of equation (C-7), equation (C-8b) may be written as

$$\left.\frac{\partial U_r}{\partial n}\right|_{z=0} = -\, R_c \left.\frac{\partial U_i}{\partial n}\right|_{z=0} . \tag{C-11}$$

The Kirchhoff-Helmholtz approximation equation (C-9b) can thus be recast into the following well-known form (Bleistein, 1984)

$$\left.\frac{\partial U_r}{\partial n}\right|_{R} = -\, R_c \left.\frac{\partial U_i}{\partial n}\right|_{R} . \tag{C-12}$$

Note that equations (C-9a) and (C-12) for $R_c = -1$ are known as the "Physical Optics Approximation for perfectly soft scatterers" or "Dirichlet boundary conditions" and for $R_c = 1$ as the "Physical Optics Approximation for perfectly rigid scatterers" or "Neumann boundary conditions." For arbitrary R_c, they are often referred to as "Kichhoff-Helmholtz approximation" implicitly assuming, however, that *monotypical reflections* are considered. The Kirchhoff-Helmholtz approximation for arbitrary reflected or transmitted (scalar) waves, may they be converted or not, is given by equations (C-9).

APPENDIX D

The isotropic scalar Kirchhoff-Helmholtz integral for elementary elastic waves derived from the general anisotropic representation theorem

We first derive the full elastic, anisotropic Kirchhoff integral. For that purpose, we start from the following two Helmholtz equations for the Green's functions $\check{\mathcal{G}}_{in}(\hat{\boldsymbol{r}},\omega;\hat{\boldsymbol{r}}_S)$ and $\check{\mathcal{G}}_{im}(\hat{\boldsymbol{r}},\omega;\hat{\boldsymbol{r}}_G)$ in the general anisotropic case (Aki and Richards, 1980), namely

$$-\rho\omega^2\check{\mathcal{G}}_{in}(\hat{\boldsymbol{r}},\omega;\hat{\boldsymbol{r}}_S) - \Big(c_{ijkl}\check{\mathcal{G}}_{kn,l}(\hat{\boldsymbol{r}},\omega;\hat{\boldsymbol{r}}_S)\Big)_{,j} = 4\pi\delta_{in}\delta(\hat{\boldsymbol{r}}-\hat{\boldsymbol{r}}^s) \; , \tag{D-1a}$$

$$-\rho\omega^2\check{\mathcal{G}}_{im}(\hat{\boldsymbol{r}},\omega;\hat{\boldsymbol{r}}_G) - \Big(c_{ijkl}\check{\mathcal{G}}_{km,l}(\hat{\boldsymbol{r}},\omega;\hat{\boldsymbol{r}}_G)\Big)_{,j} = 4\pi\delta_{im}\delta(\hat{\boldsymbol{r}}-\hat{\boldsymbol{r}}^r) \; , \tag{D-1b}$$

where $\underset{\sim}{\boldsymbol{c}}$ with components c_{ijkl} is the general anisotropic elastic tensor and $\underset{\sim}{\boldsymbol{G}}$ is the anisotropic Green's function which is also a tensor.

Using the divergence theorem that formulates the relationship between a surface integral I_S and a volume integral I_V, we may write according to Aki and Richards (1980) or Frazer and Sen (1985):

$$\begin{aligned} I_S &= \int_{\partial V}\Big(c_{ijkl}\check{\mathcal{G}}_{km,l}(\hat{\boldsymbol{r}},\omega;\hat{\boldsymbol{r}}_G)\check{\mathcal{G}}_{in}(\hat{\boldsymbol{r}},\omega;\hat{\boldsymbol{r}}_S) - c_{ijkl}\check{\mathcal{G}}_{kn,l}(\hat{\boldsymbol{r}},\omega;\hat{\boldsymbol{r}}_S)\check{\mathcal{G}}_{im}(\hat{\boldsymbol{r}},\omega;\hat{\boldsymbol{r}}_G)\Big)\, n_j \, d\hat{\boldsymbol{r}} = \\ &= \int_{V}\Big(c_{ijkl}\check{\mathcal{G}}_{km,l}(\hat{\boldsymbol{r}},\omega;\hat{\boldsymbol{r}}_G)\check{\mathcal{G}}_{in}(\hat{\boldsymbol{r}},\omega;\hat{\boldsymbol{r}}_S) - c_{ijkl}\check{\mathcal{G}}_{kn,l}(\hat{\boldsymbol{r}},\omega;\hat{\boldsymbol{r}}_S)\check{\mathcal{G}}_{im}(\hat{\boldsymbol{r}},\omega;\hat{\boldsymbol{r}}_G)\Big)_{,j} \, d\hat{\boldsymbol{r}} = I_V \; . \end{aligned} \tag{D-2}$$

The volume V is assumed to contain the source as well as the receiver, but not the scattering points. Applying the chain rule, we can recast the volume integral into the form

$$\begin{aligned} I_V &= \int_V \Big[\Big(c_{ijkl}\check{\mathcal{G}}_{km,l}(\hat{\boldsymbol{r}},\omega;\hat{\boldsymbol{r}}_G)\Big)_{,j}\check{\mathcal{G}}_{in}(\hat{\boldsymbol{r}},\omega;\hat{\boldsymbol{r}}_S) + c_{ijkl}\check{\mathcal{G}}_{km,l}(\hat{\boldsymbol{r}},\omega;\hat{\boldsymbol{r}}_G)\check{\mathcal{G}}_{in,j}(\hat{\boldsymbol{r}},\omega;\hat{\boldsymbol{r}}_S) - \\ &\quad - \Big(c_{ijkl}\check{\mathcal{G}}_{kn,l}(\hat{\boldsymbol{r}},\omega;\hat{\boldsymbol{r}}_S)\Big)_{,j}\check{\mathcal{G}}_{im}(\hat{\boldsymbol{r}},\omega;\hat{\boldsymbol{r}}_G) - c_{ijkl}\check{\mathcal{G}}_{kn,l}(\hat{\boldsymbol{r}},\omega;\hat{\boldsymbol{r}}_S)\check{\mathcal{G}}_{im,j}(\hat{\boldsymbol{r}},\omega;\hat{\boldsymbol{r}}_G)\Big] \, d\hat{\boldsymbol{r}} \; . \end{aligned} \tag{D-3}$$

We now make use of the wave equations (D-1) to replace the first and the third term in the above integral. Also, we rename the summation indices in the fourth term. We arrive at

$$\begin{aligned} I_V = \int_V \Big[&-4\pi\delta_{im}\delta(\hat{\boldsymbol{r}}-\hat{\boldsymbol{r}}^r)\check{\mathcal{G}}_{in}(\hat{\boldsymbol{r}},\omega;\hat{\boldsymbol{r}}_S) \;-\; \rho\omega^2\check{\mathcal{G}}_{im}(\hat{\boldsymbol{r}},\omega;\hat{\boldsymbol{r}}_G)\check{\mathcal{G}}_{in}(\hat{\boldsymbol{r}},\omega;\hat{\boldsymbol{r}}_S) \\ &+ c_{ijkl}\check{\mathcal{G}}_{km,l}(\hat{\boldsymbol{r}},\omega;\hat{\boldsymbol{r}}_G)\check{\mathcal{G}}_{in,j}(\hat{\boldsymbol{r}},\omega;\hat{\boldsymbol{r}}_S) \\ &+ 4\pi\delta_{in}\delta(\hat{\boldsymbol{r}}-\hat{\boldsymbol{r}}^s)\check{\mathcal{G}}_{im}(\hat{\boldsymbol{r}},\omega;\hat{\boldsymbol{r}}_G) \;+\; \rho\omega^2\check{\mathcal{G}}_{in}(\hat{\boldsymbol{r}},\omega;\hat{\boldsymbol{r}}_S)\check{\mathcal{G}}_{im}(\hat{\boldsymbol{r}},\omega;\hat{\boldsymbol{r}}_G) \\ &- c_{klij}\check{\mathcal{G}}_{in,j}(\hat{\boldsymbol{r}},\omega;\hat{\boldsymbol{r}}_S)\check{\mathcal{G}}_{km,l}(\hat{\boldsymbol{r}},\omega;\hat{\boldsymbol{r}}_G)\Big] \, d\hat{\boldsymbol{r}} \; . \end{aligned} \tag{D-4}$$

Here, we observe that the second and fifth term of the above volume integral cancel each other. Using the symmetry of the elasticity tensor $\underset{\sim}{\boldsymbol{c}}$, we observed that also the third and sixth terms do. If $\check{\mathcal{G}}_{mn}(\hat{\boldsymbol{r}},\omega;\hat{\boldsymbol{r}}_S)$ represents a direct wavefield only, and the volume V contains both source and receiver, the above integrals over Dirac's δ-functions yield the Green's functions $G_{nm}(\hat{\boldsymbol{r}}_S, \omega; \hat{\boldsymbol{r}}_G)$ and $-\check{\mathcal{G}}_{mn}(\hat{\boldsymbol{r}}_G, \omega; \hat{\boldsymbol{r}}_S)$, respectively. Due to the symmetry relation

$$\underset{\sim}{\boldsymbol{G}}(\hat{\boldsymbol{r}}, \omega; \hat{\boldsymbol{r}}^s) = \underset{\sim}{\boldsymbol{G}}^T(\hat{\boldsymbol{r}}^s, \omega; \hat{\boldsymbol{r}}) \ , \tag{D-5}$$

these are identical and thus the above volume integral vanishes. From this, we conclude that the left-hand-side surface integral over a direct field only must vanish, too.

The situation is different, if $G_{mn}(\hat{\boldsymbol{r}}, \omega; \hat{\boldsymbol{r}}^s)$ represents a superposition of a direct and a scattered wavefield,

$$\check{\mathcal{G}}_{mn}(\hat{\boldsymbol{r}}, \omega; \hat{\boldsymbol{r}}_S) = \hat{G}^0_{mn}(\hat{\boldsymbol{r}}, \omega; \hat{\boldsymbol{r}}^s) + \check{\mathcal{G}}^s_{mn}(\hat{\boldsymbol{r}}, \omega; \hat{\boldsymbol{r}}_S) \ . \tag{D-6}$$

For the direct field, $\hat{G}^0_{mn}(\hat{\boldsymbol{r}}, \omega; \hat{\boldsymbol{r}}^s)$, the volume D again contains both source and receiver, so the above integrals over Dirac's δ-functions vanish, as does the corresponding surface integral. Hovewer. for the scattered field, $\check{\mathcal{G}}^s_{mn}(\hat{\boldsymbol{r}}, \omega; \hat{\boldsymbol{r}}_S)$, the volume D only contains the receiver, but not the sources (which are, of course, secondary sources in this case). Thus, the final result of the above volume integration is

$$I_V \ = \ - 4\pi \check{\mathcal{G}}^s_{mn}(\hat{\boldsymbol{r}}_G, \omega; \hat{\boldsymbol{r}}_S) \ . \tag{D-7}$$

We have thus found the following representation for the scattered field

$$\check{\mathcal{G}}^s_{mn}(\hat{\boldsymbol{r}}_G, \omega; \hat{\boldsymbol{r}}_S) = \frac{1}{4\pi} \int_{\partial V} \Big(c_{ijkl} \check{\mathcal{G}}^s_{kn,l}(\hat{\boldsymbol{r}}, \omega; \hat{\boldsymbol{r}}_S) \check{\mathcal{G}}_{im}(\hat{\boldsymbol{r}}, \omega; \hat{\boldsymbol{r}}_G) - c_{ijkl} \check{\mathcal{G}}_{km,l}(\hat{\boldsymbol{r}}, \omega; \hat{\boldsymbol{r}}_G) \check{\mathcal{G}}^s_{in}(\hat{\boldsymbol{r}}, \omega; \hat{\boldsymbol{r}}_S) \Big) \, n_j \, d\hat{\boldsymbol{r}} \ . \tag{D-8}$$

This is the Kirchhoff integral for the scattered field in elastic, anisotropic media (see also Aki and Richards, 1980).

Generalized Kirchhoff-Helmholtz approximation

Let the secondary sources (i.e., the scattering points) be confined to a region outside V that is separated from V by a given surface Σ. As is usually done when describing scattering by means of the Kirchhoff integral (see, e.g., Langenberg, 1986), we now extend the surface ∂V of integration to infinity wherever no scattering points are met, and else to the surface Σ. There, we cannot extend the surface ∂V further because of the assumption that the sources are outside the volume V. Again due to Sommerfeld's radiation condition, the integration over the infinity parts of the boundary ∂V does not contribute. Thus, the integration in equation (D-8) reduces to a surface integral over Σ. Note that this gives rise to a change of sign of the integral because the normal vector to the surface has now to be chosen in the opposite direction to make it point outward again if the scattering surface Σ is closed. We next replace in analogy to classical Kirchhoff-Helmholtz (high-frequency) approximation (see also Appendix C) the scattered field and its derivative at the surface Σ by the specularly reflected field *after* reflection at Σ, i.e.,

$$\check{\mathcal{G}}^s_{in}(\hat{\boldsymbol{r}}, \omega; \hat{\boldsymbol{r}}_S) \ = \ \check{\mathcal{G}}^{\rm ref}_{in}(\hat{\boldsymbol{r}}, \omega; \hat{\boldsymbol{r}}_S) \ , \tag{D-9a}$$

$$\check{\mathcal{G}}^s_{kn,l}(\hat{\boldsymbol{r}}, \omega; \hat{\boldsymbol{r}}_S) \ = \ \check{\mathcal{G}}^{\rm ref}_{kn}(\hat{\boldsymbol{r}}, \omega; \hat{\boldsymbol{r}}_S) i\omega p^{\rm ref}_l \ , \tag{D-9b}$$

as well as the receiver Green's function derivative by

$$\check{\mathcal{G}}_{km,l}(\hat{\boldsymbol{r}}, \omega; \hat{\boldsymbol{r}}_G) = \check{\mathcal{G}}_{km}(\hat{\boldsymbol{r}}, \omega; \hat{\boldsymbol{r}}_G) i\omega p^r_l \ , \tag{D-10}$$

where $p_l^{\rm ref}$ and p_l^r are the components of the slowness vectors at the scattering point of the incident ray *after* specular reflection and of the receiver ray, respectively. We then arrive at

$$\begin{aligned}\check{\mathcal{G}}^s_{mn}(\hat{\boldsymbol r},\omega;\hat{\boldsymbol r}_S) &= \frac{i\omega}{4\pi}\int_\Sigma \Big(c_{ijkl}\check{\mathcal{G}}^{\rm ref}_{kn}(\hat{\boldsymbol r},\omega;\hat{\boldsymbol r}_S)p_l^{\rm ref}\check{\mathcal{G}}_{im}(\hat{\boldsymbol r},\omega;\hat{\boldsymbol r}_G) \; - \\ &\qquad - \; c_{ijkl}\check{\mathcal{G}}_{km}(\hat{\boldsymbol r},\omega;\hat{\boldsymbol r}_G)p_l^r\check{\mathcal{G}}^{\rm ref}_{in}(\hat{\boldsymbol r},\omega;\hat{\boldsymbol r}_S)\Big)\, n_j\, d\hat{\boldsymbol r} \\ &= \frac{i\omega}{4\pi}\int_\Sigma c_{ijkl}\check{\mathcal{G}}^{\rm ref}_{kn}(\hat{\boldsymbol r},\omega;\hat{\boldsymbol r}_S)\check{\mathcal{G}}_{im}(\hat{\boldsymbol r},\omega;\hat{\boldsymbol r}_G)\left(n_jp_l^{\rm ref}-n_lp_j^r\right) d\hat{\boldsymbol r}\;, \end{aligned} \qquad \text{(D-11)}$$

where we have again made use of the symmetry of $\underset{\sim}{\boldsymbol c}$. For further approximate evaluation, we introduce the generalized zero-order ray approximation (see Appendix A) for the Green's function linking the reflector point to the receiver,

$$\check{\mathcal{G}}_{ij}(\hat{\boldsymbol r},\omega;\hat{\boldsymbol r}_G) = h_i^r(\hat{\boldsymbol r})A(\hat{\boldsymbol r},\hat{\boldsymbol r}^r)e^{i\omega\tau(\hat{\boldsymbol r},\hat{\boldsymbol r}^r)}h_j(\hat{\boldsymbol r}^r)\;, \qquad \text{(D-12a)}$$

Analogously, we describe the Green's function of the specular reflected field in ray-theoretical approximation as

$$\check{\mathcal{G}}^{\rm ref}_{ij}(\hat{\boldsymbol r},\omega;\hat{\boldsymbol r}_S) = h_i^{\rm ref}(\hat{\boldsymbol r})\,A^{\rm ref}(\hat{\boldsymbol r},\hat{\boldsymbol r}^s)e^{i\omega\tau(\hat{\boldsymbol r},\hat{\boldsymbol r}^s)}h_j(\hat{\boldsymbol r}^s)\;. \qquad \text{(D-12b)}$$

Here, the change of the polarization direction is accounted for by replacing the incoming polarization vector, $\boldsymbol h^s(\hat{\boldsymbol r})$, by the reflected one, $\boldsymbol h^{\rm ref}(\hat{\boldsymbol r})$, assumed to be known. Again in analogy to classical Kirchhoff-Helmholtz approximation (Appendix C), we now assume that the amplitude $A^{\rm ref}(\hat{\boldsymbol r},\hat{\boldsymbol r}^s)$ of the reflected Green's function $\check{\mathcal{G}}^{\rm ref}_{ij}(\hat{\boldsymbol r},\omega;\hat{\boldsymbol r}_S)$ in equation (D-12b) is approximately given by the amplitude of the incident wavefield, multiplied by the scalar isotropic plane-wave reflection coefficient R_c of the elementary reflected wave under consideration. In symbols, .

$$A^{\rm ref}(\hat{\boldsymbol r},\hat{\boldsymbol r}^s) = R_c\,A(\hat{\boldsymbol r},\hat{\boldsymbol r}^s)\;. \qquad \text{(D-13)}$$

Under these approximations, we finally have in vectorial notation

$$\begin{aligned}\underset{\sim}{\boldsymbol G}^s(\hat{\boldsymbol r}^r,\omega;\hat{\boldsymbol r}^s) &= \frac{i\omega}{4\pi}\boldsymbol h(\hat{\boldsymbol r}^r)\int_\Sigma R_c\,c_{ijkl}h_i^rh_k^{\rm ref}\left(n_jp_l^{\rm ref}-n_lp_j^r\right)\;\times \\ &\qquad \times\; A(\hat{\boldsymbol r},\hat{\boldsymbol r}^r)A(\hat{\boldsymbol r},\hat{\boldsymbol r}^s)e^{i\omega[\tau(\hat{\boldsymbol r},\hat{\boldsymbol r}^r)+\tau(\hat{\boldsymbol r},\hat{\boldsymbol r}^s)]}d\hat{\boldsymbol r}\boldsymbol h^T(\hat{\boldsymbol r}^s)\;. \end{aligned} \qquad \text{(D-14)}$$

Here, we have assumed in analogy to conventional Kirchhoff approximation that the ampitude of the Green's function $\check{\mathcal{G}}^{\rm ref}_{im}(\hat{\boldsymbol r},\omega;\hat{\boldsymbol r}_S)$ *after* specular reflection at Σ at $\hat{\boldsymbol r}$ is given by the amplitude of the incident field multiplied by the scalar plane-wave reflection coefficient. The kernel or *nucleus* of this anisotropic, elastic Kirchhoff-Helmholtz integral can be written as

$$\mathcal{N}_K = c_{ijkl}h_i^rh_k^{\rm ref}\left(n_jp_l^{\rm ref}-n_lp_j^r\right)\;. \qquad \text{(D-15)}$$

Let us now further study this nucleus for the case of an isotropic medium.

Kirchhoff integral nucleus for an isotropic medium

Above, we have derived the general expression for a Kirchhoff-Helmholtz integral in the anisotropic, elastic case. Here, we will reduce the nucleus of this integral (D-14) to an isotropic medium in order to be able to compare it with the nucleus of the directly derived scalar elastic

Kirchhoff integral (I.11a). The elastic tensor $\underset{\sim}{\mathbf{c}}$ is given in the isotropic case (Aki and Richards, 1980) by

$$c_{ijkl} = \lambda\delta_{ij}\delta_{kl} + \mu(\delta_{ik}\delta_{jl} + \delta_{il}\delta_{jk}). \tag{D-16}$$

Inserting this into equation (D-15), we obtain for the nucleus of the Kirchhoff integral

$$\begin{aligned} \mathcal{N}_K &= [\lambda\delta_{ij}\delta_{kl} + \mu(\delta_{ik}\delta_{jl} + \delta_{il}\delta_{jk})]h_i^r h_k^{\text{ref}}(n_j p_l^{\text{ref}} - n_l p_j^r) \\ &= [\lambda h_j^r h_l^{\text{ref}} + \mu(\delta_{jl} h_i^r h_i^{\text{ref}} + h_l^r h_j^{\text{ref}})](n_j p_l^{\text{ref}} - n_l p_j^r) \ . \end{aligned} \tag{D-17}$$

Now, we have to make a distinction between two possible cases: (a) the receiver ray is that of an elementary P-wave, and (b) the receiver ray is that of an elementary S-wave. Case (a) includes P-Pand S-Preflections, and case (b) includes P-Sand S-Sreflections.

In the case of (a), we have $h_i^\gamma = v_p p_i^\gamma$ and $h_i^\gamma p_i^\gamma = 1/v_p$, where v_p is the P-wave velocity and γ may be r or ref. Then the Kirchhoff integral nucleus becomes

$$\mathcal{N}_K = [\lambda + 2\mu(-h_i^{\text{ref}} h_i^r)](p_j^r n_j - p_j^{\text{ref}} n_j) \ . \tag{D-18}$$

In the case of (b) on the other hand, we have $h_i^\gamma p_i^\gamma = 0$. Thus, we obtain

$$\mathcal{N}_K = \mu[-h_i^r h_i^{\text{ref}}(n_j p_j^r - n_j p_j^{\text{ref}}) + h_l^r p_l^{\text{ref}} h_j^{\text{ref}} n_j - h_l^r n_l h_j^{\text{ref}} p_j^r] \ . \tag{D-19}$$

Under the further approximation that $\boldsymbol{h}^{\text{ref}} \simeq -\boldsymbol{h}^r$, which is true in the vicinity of the specular reflection point, from where the main contribution of the Kirchhoff integral stems, we can find again a common expression for the nucleus for both cases (a) and (b), namely

$$\mathcal{N}_K = \rho v^2 (p_j^r - p_j^{\text{ref}}) n_j = 2f \ \mathcal{O}_K \ , \tag{D-20}$$

where $\mathcal{O}_K$ is the obliquity factor of the Kirchhoff integral defined in equation (I.10) and $f = \rho v^2$ as defined in Appedinx A for elastic waves. Quantity v is the velocity encountered by the outgoing wavefield after scattering at the medium discontinuity, i.e., $v = v_p = \sqrt{(\lambda + 2\mu)/\rho}$ for case (a) and $v = v_s = \sqrt{\mu/\rho}$ for case (b).

The Green's function (D-14) can thus be expressed in the form

$$\underset{\sim}{\boldsymbol{G}}^s(\hat{\boldsymbol{r}}^r, \omega; \hat{\boldsymbol{r}}^s) \ = \ \boldsymbol{h}(\hat{\boldsymbol{r}}^r) U(\hat{\boldsymbol{r}}^r, \omega; \hat{\boldsymbol{r}}^s) \boldsymbol{h}^T(\hat{\boldsymbol{r}}^s) \ , \tag{D-21}$$

where the scalar quantity

$$\begin{aligned} U(\hat{\boldsymbol{r}}^r, \omega; \hat{\boldsymbol{r}}^s) \ &= \ \frac{i\omega}{4\pi} \int_\Sigma R_c c_{ijkl} h_i^r h_k^{\text{ref}} \left(n_j p_l^{\text{ref}} - n_l p_j^r\right) \times \\ &\times A(\hat{\boldsymbol{r}}, \hat{\boldsymbol{r}}^r) A(\hat{\boldsymbol{r}}, \hat{\boldsymbol{r}}^s) e^{i\omega[\tau(\hat{\boldsymbol{r}}, \hat{\boldsymbol{r}}^r) + \tau(\hat{\boldsymbol{r}}, \hat{\boldsymbol{r}}^s)]} d\hat{\boldsymbol{r}} \end{aligned} \tag{D-22}$$

can be approximated by the integral

$$U(\hat{\boldsymbol{r}}^r, \omega; \hat{\boldsymbol{r}}^s) \ = \ \frac{i\omega}{4\pi} \int_\Sigma R_c \, \rho v^2 \, (\hat{\boldsymbol{p}}^r - \hat{\boldsymbol{p}}^{\text{ref}}) \cdot \hat{\boldsymbol{n}} A(\hat{\boldsymbol{r}}, \hat{\boldsymbol{r}}^r) A(\hat{\boldsymbol{r}}, \hat{\boldsymbol{r}}^s) e^{i\omega[\tau(\hat{\boldsymbol{r}}, \hat{\boldsymbol{r}}^r) + \tau(\hat{\boldsymbol{r}}, \hat{\boldsymbol{r}}^s)]} d\hat{\boldsymbol{r}} \ . \tag{D-23}$$

This is exactly the same expression as equation (I.11a) that was independently derived in the text starting from the scalar elastic wave equation (A-8) of Appendix A.